Validating Earth and ocean tide models using tidal gravity measurements

Trevor F. Baker and Machiel S. Bos*

Proudman Oceanographic Laboratory, Bidston Observatory, Birkenhead CH43 7RA, UK. E-mail: tfb@pol.ac.uk

SUMMARY

O1 and M2 observations from well-calibrated spring gravimeters and superconducting gravimeters from the Global Geodynamics Project (GGP) are used to test models of the Earth's body tide and 10 ocean tide models. It is shown that some of the ocean tide models give anomalous results in various parts of the world. For example, the Schwiderski ocean tide model gives discrepancies in several areas and the FES series of ocean tide models have problems in the western Pacific (China, Japan and Australia). The majority of the high-quality tidal gravity measurements in Europe are in close agreement with the Dehant, Defraigne and Wahr (DDW) elastic and inelastic body tide models. The gravimetric factors for the DDW elastic and inelastic models only differ by 0.12 per cent and the present calibration accuracy does not allow us to distinguish between these models, but does reduce the previous upper bound on inelastic gravimetric factors. The European observations give a phase lag of a few hundredths of a degree for the O1 body gravity tide, which is consistent with the Mathews inelastic body tide model. At some European and worldwide stations the gravimetric factors differ by up to 0.3 per cent from the DDW model and it is suggested that further checks on the gravimeter calibrations are required. Accurate determinations of instrumental phase lags are now easier to achieve and the imaginary (out-of-phase) component of tidal gravity can be used for accurate tests of this component of ocean tide models.

Key words: Earth tides, gravity, ocean tides, tides.

1 INTRODUCTION

The interpretation of tidal gravity measurements has always been closely linked with the improvement of ocean tide models. When ocean tide models were relatively poor, it was usually assumed that the Earth's body tide was well known from Earth models available from seismology. The tidal gravity body tide for a particular tidal harmonic was then subtracted from the observed tidal gravity harmonic in order to test the ocean tide models (e.g. Farrell 1972b; Baker 1980). Later, with the improvement of ocean tide models following the availability of TOPEX/POSEIDON altimetry data, tidal gravity measurements at sites at large distances from the ocean and therefore with a relatively small ocean tide loading, were used for testing body tide models (Baker *et al.* 1996). In the present work we use tidal gravity observations from spring gravimeters and superconducting gravimeters from the Global Geodynamics Project (Crossley *et al.* 1999; Hinderer & Crossley 2000), at various distances from the oceans, to test the latest body and ocean tide models. In the next two sections we briefly summarize these model developments.

Most of the available tidal gravity observations are from mid-latitude stations. At these latitudes the O1 body tide amplitude is typically in the range 25–35 μGal and the M2 body tide amplitude is typically in the range 20–70 μGal. Since the ocean tide loading is normally only a few tenths of a μGal up to 3 μGal, it is usually a small fraction of the total signal. This means that any observational error caused by the gravimeter calibration or phase lag determination may be a small fraction of the total signal, but is considerably amplified as a fraction of the ocean tide loading component. In general, in order to provide useful tests of ocean tide models, a calibration accuracy of 0.1 per cent is required and an equivalent accuracy for the phase lag determination, which is 0.057°. The semi-diurnal body tide amplitudes are zero at the poles and the diurnal body tide amplitudes are zero at the poles and the equator. Near these specific latitudes, the gravimeter calibration is not so critical and useful tests of ocean tide models can be made even with a calibration uncertainty of the order of 1 per cent (Agnew 1995; Bos *et al.* 2002).

Wahr & Bergen (1986) showed that dispersion of the Love numbers arising from the Earth's inelasticity could increase the semi-diurnal and diurnal gravimetric factors by at most 0.36 per cent. It therefore follows that a calibration accuracy of 0.1 per cent, or better, is also required for testing body tide models (see Section 2). Most of the tidal gravity observations in the International Centre for Earth

*Now at: DEOS, Thijsseweg 11, 2629 JA Delft, The Netherlands.

Tides (ICET) databank (Melchior 1994) were made with astatized spring gravimeters and have a calibration uncertainty of the order of ±1 per cent (see Melchior & Francis 1998) for a recent review of tidal gravity observations in the ICET databank). The errors of the majority of observations in the ICET databank are an important limitation when trying to use the databank for testing ocean tide models. Llubes & Mazzega (1997) and Melchior & Francis (1996) found that unexplained residuals, with standard deviations of the order of 0.3–0.6 µGal for O1 and M2, remained after using various ocean tide models for the ocean tide loading computations. Many of the problems with astatized gravimeters are caused by hysteresis and a sensitivity that depends critically upon tilts of the gravimeter along the direction of the mass. These problems can be avoided by continuously nulling the mass using electrostatic feedback. Because of the importance of calibration for both spring and superconducting gravimeters, calibration methods are reviewed in Section 4.

2 BODY TIDE MODELS

The latest models of the Earth's body tides use the radial profiles of the spherically averaged density and elastic parameters of the Preliminary Reference Earth Model (PREM) of Dziewonski & Anderson (1981). The body tide computed for an ellipsoidal, rotating Earth in hydrostatic equilibrium using the PREM model (with modification of the surface layer) was used as a benchmark for intercomparison of different computer models and resolving the previous discrepancies between the results of different modellers (Dehant 1998). Dehant *et al.* (1999) give Love numbers and gravimetric factors for this elastic, hydrostatic model and we call this the DDW elastic model. They also give model results for an inelastic, non-hydrostatic model (called henceforth the DDW inelastic model). In this model they increased the flattening of the core–mantle boundary by 500 m in order to obtain a frequency for the free core nutation that is in agreement with observations of luni-solar nutations and tidal gravity measurements. Over the past few years, the measurements of the tidal gravity harmonics near K1 have been used to determine the period and damping of the free core nutation (for a recent review of these measurements see Hinderer & Crossley 2000).

There is considerable interest in determining the inelasticity of the Earth at tidal periods, but observational evidence is very limited (Wahr & Bergen 1986). Usually a seismic Q model is used and it is assumed that Q varies with frequency to the power α between a reference period and tidal periods. Neither the reference period nor the value of α are well constrained by observations. Dehant *et al.* (1999) and Mathews *et al.* (1997) use the seismic Q values at 300 s from the model of Widmer *et al.* (1991) and $\alpha = 0.15$. Mathews *et al.* (1997) also show the effects on the Love numbers of using a range of values of α and reference periods of 1, 200 and 300 s. Baker *et al.* (1996) showed that an earlier body tide model of Dehant, using a Q model with a reference period of 1 s and $\alpha = 0.15$, gave an increase in the gravimetric factor that was too large to be consistent with tidal gravity observations in central Europe.

Models have been developed that allow for departures from laterally homogeneous, layered Earth models. Wang (1991) and Kopaev & Kuznetsov (2000) used models for lateral heterogeneities up to degree and order eight from seismic tomography. They found that the departures of the gravimetric factors from those for the PREM model are only up to a maximum of ±0.05 per cent. Only for the case where there is very significant amplification owing to dispersion between seismic and tidal frequencies can the effects be of the order of 0.1 µGal (Wang 1991). Although claims have been made

that some tidal gravity observations show evidence of the effects of lateral heterogeneities or correlations with heat flow, this evidence has been strongly disputed (see Zürn 1997, for a recent review).

3 OCEAN TIDE MODELS

Numerical models of ocean tides using Laplace's tidal equations, and including the effects of friction, ocean self-attraction and the loading deformation of the ocean bottom were extensively developed from the late 1960s to 1980. However, these models were only in general qualitative agreement with ocean tide observations and were not accurate enough for use in geophysical work. This was mainly caused by the models having only a relatively coarse resolution (e.g. 1 × 1 deg) and therefore inadequately modelling the main areas of tidal dissipation in shallow seas. In order to improve the ocean tide models, it was necessary to constrain them to fit coastal tide gauge observations. The 1 × 1 deg ocean tide model of Schwiderski (1980) used a method called hydrodynamic interpolation in order to constrain the model to a large number of coastal and island tide gauge observations and some ocean bottom tide gauges. The Schwiderski (SCHW) model solutions have been used as a standard in geophysical work for many years and hence have been used in the present work.

The problem of resolution of numerical ocean tide models led to the development of finite-element hydrodynamic models. Le Provost *et al.* (1994) developed the FES94.1 model, which used a finite-element mesh of 200 km in the deep ocean reducing to 10 km in coastal areas. The FES94.1 model is only constrained by observations at ocean domain boundaries, but gives an improved agreement with tide gauge observations in many areas compared with the Schwiderski model. Nevertheless, the availability of precise altimetry data from the TOPEX/POSEIDON (T/P) satellite showed that FES94.1 had broad scale errors in several areas of the deep ocean. Once again this led to the development of ocean tide models constrained by observations (satellite altimetry and/or tide gauges). Over the next few years many new ocean tide models were developed using the TOPEX/POSEIDON observations (for a recent review see Le Provost 2001).

The University of Texas ocean tide model CSR3.0 (Eanes & Bettadpur 1996) uses a response analysis of 2.4 yr of T/P data to find long-wavelength corrections to the FES94 hydrodynamic model. The model is available on a 0.5 × 0.5 deg grid and so preserves the fine details of the FES94.1 model, whilst being more accurate at longer wavelengths. CSR4.0 is a recent update of this model using a longer T/P data set. Outside the ±66° latitudes covered by T/P, these models default to the FES94.1 solution. FES95.2 (Le Provost *et al.* 1998) assimilates (using a representer approach) an earlier version of the Texas altimetry solution (CSR2.0), sampled for ocean depths greater than 1000 m, into the FES94.1 model. Accuracy tests show that the tidal models that use T/P altimetry data agree with *in situ* observations in the deep ocean to within a few centimetres for the total tide (Le Provost 2001). However, in shallow areas differences between the models can be over 50 cm. The spacing of the altimeter ground tracks (2.83°) makes it more difficult to accurately extract the tides over the shallow areas where the tides are larger and the spatial scales much smaller than in the deep ocean. Lefèvre *et al.* (2000a) therefore developed an improved finite-element model, FES98, which assimilated harmonics from approximately 700 coastal, island and deep ocean tide gauges. The model is completely independent of satellite altimetry data and is more accurate on the continental shelves than the previous FES

models (the rms against a largely independent set of 727 coastal tide gauges is 11 cm for M2 compared with 22 cm for FES95.2). The new FES99 model (Lefèvre *et al.* 2002) computes five semi-diurnal and three diurnal harmonics using the representer method to assimilate observations from approximately 700 coastal tide gauges and 687 T/P altimeter crossover points in the deep ocean. An unconstrained version of the hydrodynamic finite-element model disagrees with open ocean tide gauge measurements by 30–40 per cent for these harmonics, which shows the necessity of assimilating altimetry and tide gauge data. Accuracy tests show that FES99 is more accurate than the previous FES models, both in the deep oceans and along the global coastlines (Lefèvre *et al.* 2002).

TPXO.5 is the latest version of the ocean tide model of Egbert *et al.* (1994). This model uses the linearized hydrodynamic equations and the representer method to assimilate T/P crossover data. The GOT99.2b ocean tide model (Ray 1999) uses harmonic analysis of 6 yr of T/P altimetry data to give corrections to a 0.5×0.5 deg prior model. The major part of the prior model is the FES94.1 hydrodynamic model (as is the case for the CSR3.0 and CSR4.0 models) but this is supplemented by local tidal models in the Gulf of Maine and Gulf of St Lawrence, the Persian Gulf and the Mediterranean and Red Seas. The NAO99b ocean tide model (Matsumoto *et al.* 2000) assimilated 5 yr of T/P data into a 0.5×0.5 deg global hydrodynamic model. Special attention was given to obtaining improved solutions in shallow areas by tidal analysis of T/P altimeter data in $0.5°$ bins along the ground tracks. These were then assimilated into the hydrodynamic model at each time step using a blending method. Tests using shallow water tide gauges and altimeter residuals were then used to show that NAO99b is more accurate in shallow seas than CSR4.0 or GOT99.2b.

4 CALIBRATION OF TIDAL GRAVIMETERS

In Section 1 it was shown that accurate amplitude and phase calibrations of tidal gravimeters are essential in using the observations for testing ocean tide or body tide models. Moore & Farrell (1970) pointed out that an amplitude calibration accuracy of 0.1 per cent is required, but many of the observations over the past 30 yr have failed to achieve this accuracy. Calibration of instrumental phase lags is equally important (on a phasor plot a $0.057°$ error in phase is equivalent to a 0.1 per cent error in amplitude), but this has not always received sufficient attention. For these levels of accuracy, the manufacturer's calibrations are insufficient. Even the LaCoste and Romberg ET (LCR ET) continuously nulling gravimeters, which were specifically designed for Earth tide measurements, do not meet the required accuracy. Baker (1980) showed that the measuring screw calibrations of LCR ET13 and ET15 differed by 0.5 per cent. In order to improve the accuracy of the measuring screw calibrations to 0.1 per cent, ET13, ET15 and ET10 were recalibrated on the vertical calibration line at the University of Hannover (Baker *et al.* 1989, 1991). This line is in a 19 storey building and was set up using many LCR G and D gravimeters and tied into absolute gravity stations (Kanngiesser & Torge 1981). Tidal gravity observations with ET13 and ET15 in Europe were then used to show that the 'standard' calibration used by the International Centre for Earth Tides (ICET) for worldwide tidal gravity measurements was 1.2 per cent too high. This led to the renormalization of the 305 worldwide tidal gravity observations in the ICET databank, but the calibration/sensitivity errors at individual stations are still of the order of ± 1 per cent (Melchior 1994).

Superconducting gravimeters are very precise instruments, but their output is in volts and therefore an accurate calibration of the amplitude (and phase) is still required. In general these instruments are not portable enough for measuring on calibration lines. This has led to the development of *in situ* calibration methods (Richter 1995). The method that has received the most attention over the past few years and is now used at most GGP stations is parallel recording with an absolute gravimeter. Originally the JILAG absolute gravimeters were used, but the results were only accurate to between 0.3 and 1 per cent (Hinderer & Crossley 2000). However, the development of the new FG5 absolute gravimeter has now allowed improved accuracies to be achieved. Francis *et al.* (1998) used 9 d of parallel recording of an FG5 absolute gravimeter and a superconducting gravimeter at the quiet site at Table Mountain Gravity Observatory near Boulder, USA to show that at least 5 d of observations are required in order to achieve an accuracy of 0.1 per cent. However, in a recent review Meurers (2001) showed that most of the reported calibration accuracies using absolute gravimeters at superconducting gravimeter stations are in the range 0.1–0.4 per cent.

Experiments have been performed with large moving masses for calibration of both LCR and superconducting gravimeters (Richter 1995). A 273 kg mass in the form of a ring, which produces a gravity change of 6.7 µGal, has been used to calibrate the superconducting gravimeter at Brasimone in Italy to an accuracy of 0.3 per cent (Achilli *et al.* 1995). A sinusoidal acceleration system for calibrating LCR and superconducting gravimeters has been developed (Richter *et al.* 1995). The foot screws of the superconducting gravimeter are driven through a range of 20 mm with periods from 200 to 2400 s with careful control using a digital feedback system. The calibration factor at zero frequency can then be found to an accuracy of 0.1 per cent (Richter *et al.* 1995). The sinusoidal acceleration system has been used for calibrating the dual-sphere superconducting gravimeter SG CD029 at Wettzell (Harnisch *et al.* 2000) and SG C024 at Boulder. The calibration of SG C024 using the parallel recording with the FG5 absolute gravimeter agrees with the calibration using the acceleration system to within 0.1 per cent (Francis *et al.* 1998).

In recent years improved methods for determining the instrumental phase lags arising from the feedback, filters and data acquisition system have been developed (Wenzel 1994). Either step functions or sine wave voltages are injected into the feedback loop in order to find the transfer function of the instrument. Van Camp *et al.* (2000) performed experiments on the superconducting gravimeter at Membach, Belgium, and showed that the time lags could be determined to an accuracy of 0.01 s, which is equivalent to better than $0.0001°$ at semi-diurnal periods.

5 EUROPEAN RESULTS: SPRING GRAVIMETERS

5.1 Observations

Compared with other continents, a very large number of tidal gravity observations are available in Europe. However, there are very few available with a clearly documented account of the methods used and accuracies achieved for independent checks on calibrations and on instrumental phase lags. For the present work, observations from eight sites in central Europe have been used (see Table 1). The table shows the gravimeters used at each site and the calibration lines that were used in order to improve the calibrations. The references shown should be consulted in order to obtain full information on the measurements, including calibration and sensitivity tests, phase lag

Table 1. European spring gravimeter stations.

Site	Gravimeter	Calibration line	Reference
Chur	ET13	Hannover	Baker *et al.* (1991)
Zurich	ET13	Hannover	Baker *et al.* (1991)
Schiltach	ET19	Hannover	Wenzel *et al.* (1991)
Karlsruhe	G156/249SRW	Hannover	Wenzel (1996)
B. Homburg	ET15	Hannover & Wuhan	Baker *et al.* (1991)
Pecny	A GS15-228	Czech	Broz & Simon (1997)
Hannover	G/D SRW	Hannover & Hornisgrinde	Timmen & Wenzel (1994)
Potsdam	ET16	Wuhan	Dittfeld *et al.* (1993)

determinations and the associated errors. The observations at Chur, Zurich and Bad Homburg are described in Baker *et al.* (1989) and more fully in Baker *et al.* (1991). The measurements were made with LCR ET13 and ET15, which had earlier been converted to continuously nulling gravimeters using electrostatic feedback. As discussed above, the manufacturer's measuring screw calibrations were improved to an accuracy of 0.1 per cent using the vertical calibration line at Hannover. The calibration of ET15 was also confirmed to within 0.1 per cent using the 5.7 mGal vertical baseline at the Institute of Geodesy and Geophysics in Wuhan, China (Hsu *et al.* 1991).

Observations made with two other LCR ET gravimeters with electrostatic feedback were also used in the present work (Table 1). ET19 at the Black Forest Observatory, Schiltach, Germany, was calibrated using parallel recording with two feedback gravimeters, which had been calibrated on the Hannover vertical baseline (Wenzel *et al.* 1991). The measurements at Potsdam were made with ET16 following its recalibration on the Wuhan vertical baseline (Dittfeld *et al.* 1993).

The tidal gravity observations at Hannover were made with three LCR model G gravimeters (079, 087 and 995) and LCR D014, which had all been converted to continuously nulling gravimeters using SRW electrostatic feedback (Timmen & Wenzel 1994). These gravimeters were again calibrated on the Hannover vertical baseline. In addition, Timmen & Wenzel (1994) used tidal gravity observations made with LCR G299 with electromagnetic feedback. This instrument had been calibrated on the independent Hornisgrinde, Black Forest, baseline that was set up using absolute gravimeters. The tidal gravity observations at Karlsruhe (Wenzel 1996) were made using LCR G156 and G249, which have SRW electrostatic feedback systems and were calibrated on the Hannover vertical baseline.

We also use the observations at Pecny, Czech Republic, made with the Askania gravimeter Gs15-228 (Broz & Simon 1997). This

gravimeter was equipped with a new digital recording system, which eliminated the phase lag arising from the analogue recording of the observations that we used in our previous paper (Baker *et al.* 1996). The gravimeter was calibrated on the Czech gravity baseline and a very careful series of tests were made in order to eliminate the internal non-linearities that normally affect observations with these gravimeters (Simon & Broz 1993).

From Table 1 it can be seen that altogether four different gravimeter calibration lines have been used in order to improve the manufacturer's calibrations of the gravimeters used in the present work. The typical error in the calibrations given in the above papers is ±0.1 per cent rms. The rms noise errors as determined from least-squares tidal analyses are typically ±0.04 per cent (±0.02°) for M2 and ±0.07 per cent (±0.04°) for O1. The total rms errors are of the order of ±0.12 per cent for the M2 and O1 amplitudes. The instrumental phase lags caused by the feedback and filters are normally determined using step response tests and the errors in determining these phase lags are combined with the above noise errors in order to give the total phase errors. The quoted total rms phase errors are typically in the range ±0.03°–0.05°.

5.2 Testing body and ocean tide models

The observed O1 and M2 gravimetric factors and phases for the eight central European sites are given in Tables 2 and 3. In order to test the latest models of the Earth's body tide, the observations have to be corrected for ocean tide loading and attraction. Over the past few years many new ocean tide models have become available (see Section 3). We have used nine of these new models (plus the Schwiderski ocean tide model, which was used as a standard for many years). The range of ocean tide models allows an assessment to be made of the effects of the remaining uncertainties in ocean tides on the corrected observed gravimetric factors. The ocean tide model for a particular tidal harmonic is convolved with the Green's

Table 2. O_1 gravimetric factors and phases: observed and observed corrected using three recent ocean tide models (local phases, in brackets, in degrees with lags negative).

Site	O_1 observed	Corrected using GOT 99.2b	Corrected using NAO 99b	Corrected using FES 99
Chur	1.1473 (0.02)	1.1514 (−0.09)	1.1512 (−0.11)	1.1517 (−0.07)
Zurich	1.1477 (0.02)	1.1520 (−0.08)	1.1518 (−0.10)	1.1522 (−0.07)
Schiltach	1.1470 (0.07)	1.1513 (−0.04)	1.1512 (−0.06)	1.1515 (−0.02)
Karlsruhe	1.1485 (0.09)	1.1527 (−0.03)	1.1526 (−0.05)	1.1530 (−0.01)
B. Homburg	1.1478 (0.06)	1.1519 (−0.07)	1.1518 (−0.09)	1.1521 (−0.06)
Pecny	1.1491 (0.09)	1.1528 (−0.04)	1.1528 (−0.06)	1.1532 (−0.03)
Hannover	1.1499 (0.15)	1.1537 (0.01)	1.1536 (−0.02)	1.1540 (0.01)
Potsdam	1.1477 (0.17)	1.1517 (0.01)	1.1517 (−0.01)	1.1520 (0.02)
	Mean	1.1522 (−0.04)	1.1521 (−0.06)	1.1525 (−0.03)
	Std. dev.	0.0008 (0.04)	0.0008 (0.04)	0.0009 (0.04)

Table 3. M$_2$ gravimetric factors and phases: observed and observed corrected using three recent ocean tide models (local phases in degrees, lags negative).

Site	M$_2$ observed	Corrected using GOT 99.2b	Corrected using NAO 99b	Corrected using FES 99
Chur	1.1828 (1.74)	1.1598 (−0.02)	1.1600 (0.00)	1.1601 (−0.03)
Zurich	1.1842 (1.86)	1.1601 (−0.10)	1.1603 (−0.07)	1.1605 (−0.11)
Schiltach	1.1848 (2.06)	1.1596 (0.04)	1.1596 (0.09)	1.1600 (0.05)
Karlsruhe	1.1868 (2.02)	1.1610 (0.02)	1.1610 (0.07)	1.1616 (0.03)
B. Homburg	1.1869 (1.96)	1.1602 (0.00)	1.1601 (0.07)	1.1612 (0.03)
Pecny	1.1839 (1.22)	1.1609 (0.00)	1.1609 (0.02)	1.1613 (0.00)
Hannover	1.1865 (1.68)	1.1617 (−0.02)	1.1617 (0.13)	1.1638 (0.08)
Postdam	1.1845 (1.39)	1.1606 (0.02)	1.1604 (0.06)	1.1615 (0.03)
Mean		1.1605 (−0.01)	1.1605 (0.05)	1.1613 (0.01)
Std. dev.		0.0007 (0.04)	0.0007 (0.06)	0.0012 (0.06)

function, G, for the Preliminary Reference Earth Model to give the ocean tide loading (plus attraction), $\mathbf{L}$, at the gravity station, which has a position vector $\mathbf{r}$, i.e.

$$\mathbf{L}(\mathbf{r}) = \rho \iint G(|\mathbf{r} - \mathbf{r}'|)\mathbf{Z}(\mathbf{r}')\,d\mathrm{A} \qquad (1)$$

This is a global integral over the surface of the oceans, where ρ is the density of sea water and $\mathbf{Z}$ is the ocean tide amplitude at position vector $\mathbf{r}'$. Since the ocean tide harmonic is periodic, it is convenient to use a complex ocean tide amplitude $\mathbf{Z}$ (and complex loading $\mathbf{L}$). The real component of eq. (1) is then the part that is in phase with the tidal potential and the imaginary component is the part in quadrature (out of phase) with the tidal potential. The gravity Green's function, G, has three components: the direct Newtonian attraction of the ocean tide mass; the change in gravity arising from the vertical displacement of the gravity station; and the change in the Earth's gravity field owing to the redistribution of mass in the Earth (Farrell 1972a).

The M2 and O1 observed gravimetric factors corrected for ocean tide loading and attraction using the 10 different ocean tide models are shown in Fig. 1 and the corresponding corrected phases are shown in Fig. 2. The theoretical gravimetric factors for the DDW elastic PREM model and the DDW non-hydrostatic inelastic model (Dehant *et al.* 1999) are shown in Fig. 1. The inelastic model uses
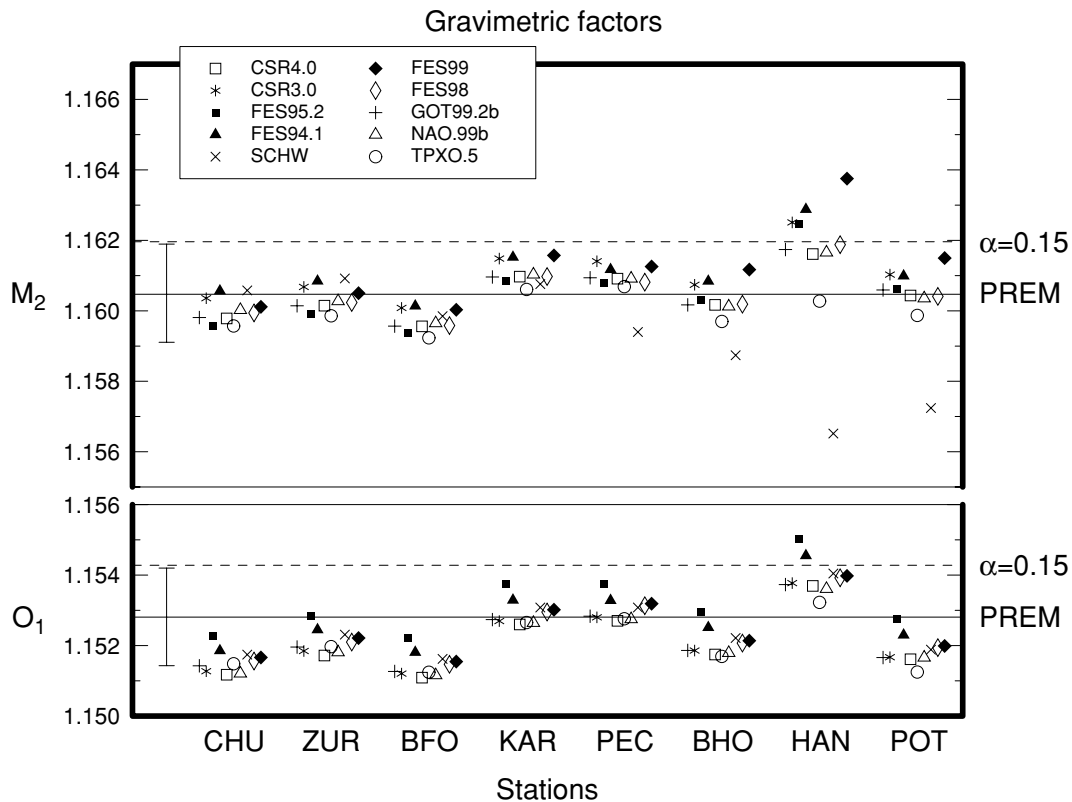

Figure 1. M2 and O1 observed gravimetric factors corrected for ocean tide loading and attraction using 10 different ocean tide models. The theoretical body tide gravimetric factors are shown for the DDW elastic PREM model and the DDW inelastic model (with $\alpha = 0.15$). The observations are from the following sites: Chur (CHU) and Zurich (ZUR) in Switzerland; Black Forest Observatory, Schiltach (BFO), Karlsruhe (KAR), Bad Homburg (BHO), Hannover (HAN) and Potsdam (POT) in Germany; Pecny (PEC), Czech Republic.
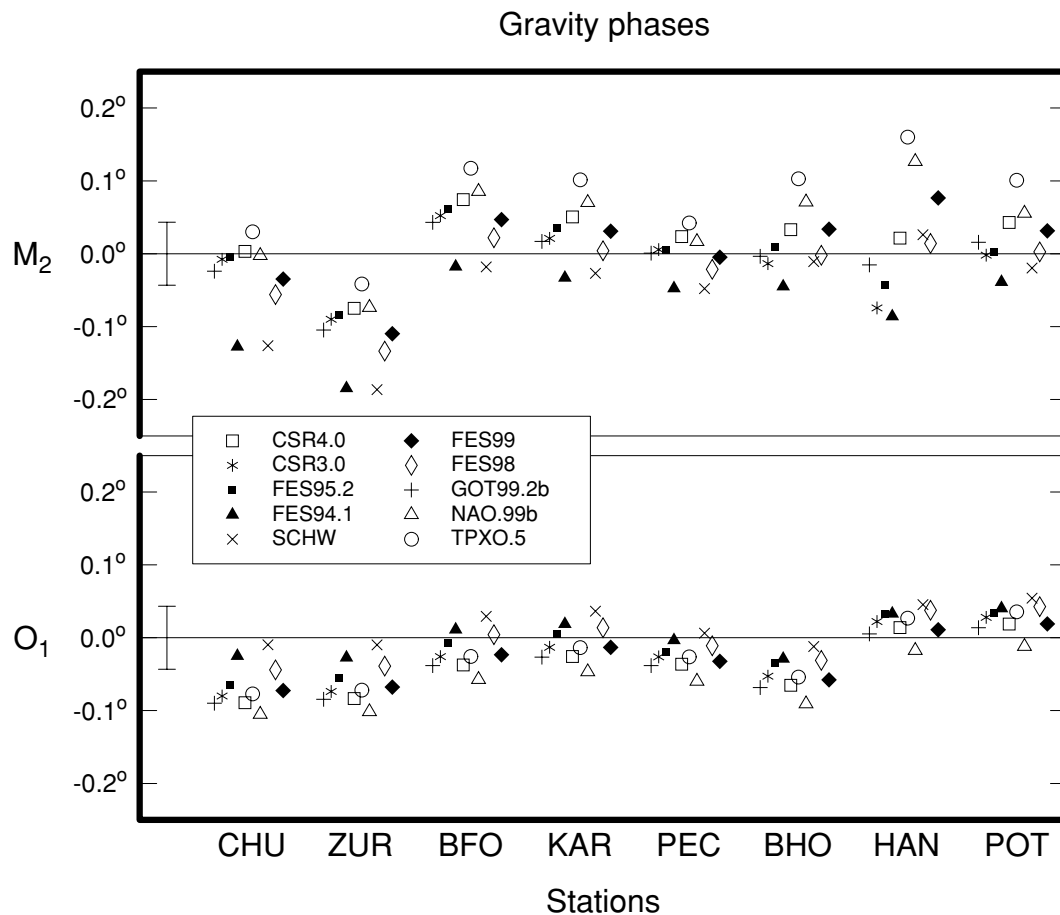
Gravity phases

Figure 2. M2 and O1 observed phases corrected for ocean tide loading and attraction using 10 different ocean tide models. The phases are with respect to the tidal potential in the local meridian and phase leads are positive.

a frequency to the power αQ model, with $\alpha = 0.15$ and the Q model of Widmer *et al.* (1991) at the reference period of 300 s. It can be seen that the inelastic model only increases the gravimetric factors by 0.12 per cent. It should be noted that this is significantly less than the corresponding increase shown in our previous paper (Baker *et al.* 1996), which showed the results from a preliminary version of the Dehant model, which used a reference period of 1 s for the Q model. The effect of inelasticity is of the same order as the calibration errors (typical observational error bars are shown on the left-hand side of Fig. 1). These observations can be used to reject models that give increases in the gravimetric factors owing to inelasticity near the upper bounds found by Wahr & Bergen (1986), i.e. over 0.3 per cent, but cannot be used to distinguish between the elastic and inelastic models used here.

Tables 2 and 3 give the corrected gravimetric factors using three of the most recent ocean tide models, GOT99.2b, NAO99b and FES99. The tables also show the mean O1- and M2-corrected gravimetric factors over the eight sites and the standard deviations. These standard deviations are of the same order as the above estimated calibration errors. The mean O1 gravimetric factors are in the range 1.1521–1.1525, whereas at these latitudes the DDW elastic O1 gravimetric factor is 1.1528 and the inelastic factor is 1.1543. The mean M2 gravimetric factors are in the range 1.1605–1.1613, whereas the DDW models give 1.1605 and 1.1619 for the elastic and inelastic models, respectively.

In Fig. 1, the Schwiderski M2 ocean tide model clearly gives anomalous results for Pecny, Bad Homburg, Hannover and Potsdam compared with the other ocean tide models. This is caused by the inadequate resolution of this 1×1 deg model in the North Sea and the English Channel. It should be noted that in previous work we have replaced the Schwiderski model with a regional model of the tides on the northwestern European shelf. However, many published papers have used the Schwiderski ocean tide model and the results shown here illustrate the problems with using this model, even for stations in central Europe at relatively large distances from the coast.

Figs 1 and 2 show that the Hannover M2-corrected amplitudes and phases are relatively sensitive to the choice of ocean tide model. This station is only approximately 170 km from the North Sea and therefore the Hannover M2 results are not suitable for testing models of the Earth's body tides. At all of the European tidal gravity stations the remaining uncertainties in the M2 ocean tides are more significant than is the case for the O1 ocean tide uncertainties. This is particularly clear in Fig. 2, where it can be seen that the corrected M2 phases using different ocean tide models have a greater spread than the corresponding corrected O1 phases. This is caused by the very small O1 ocean tide loading in central Europe, ~0.15 μGal, which is approximately a factor of 10 smaller than the M2 ocean tide loading. The spread of corrected M2 phases in Fig. 2 can be used to assess the various M2 ocean tide models. At all of the stations in Germany it can be seen that TPXO.5 and NAO99b give corrected M2 phase leads that are too high. The results for Hannover also show that FES94.1 gives a corrected phase lag that is too high. The results from the superconducting gravimeters in Europe, which will

Table 4. O$_1$ gravimetric factors and phases: observed and observed corrected using three recent ocean tide models (local phases in degrees, lags negative).

Site	O$_1$ observed	Corrected using GOT 99.2b	Corrected using NAO 99b	Corrected using FES 99
Brasimone	1.1460 (0.06)	1.1498 (−0.09)	1.1493 (−0.10)	1.1500 (−0.07)
Medicina	1.1493 (0.17)	1.1535 (0.00)	1.1528 (−0.01)	1.1537 (0.03)
Vienna	1.1479 (0.10)	1.1516 (−0.02)	1.1515 (−0.05)	1.1519 (−0.02)
Strasbourg	1.1490 (0.08)	1.1533 (−0.03)	1.1533 (−0.05)	1.1536 (−0.01)
Wettzell (lo)	1.1485 (0.08)	1.1523 (−0.04)	1.1522 (−0.06)	1.1527 (−0.03)
Wettzell (up)	1.1500 (0.09)	1.1538 (−0.03)	1.1537 (−0.05)	1.1541 (−0.03)
Membach	1.1511 (0.07)	1.1550 (−0.07)	1.1550 (−0.09)	1.1552 (−0.05)
Brussels	1.1533 (0.06)	1.1568 (−0.09)	1.1568 (−0.13)	1.1569 (−0.07)
Potsdam	1.1498 (0.13)	1.1537 (−0.02)	1.1537 (−0.05)	1.1541 (−0.02)
Metsähovi	1.1532 (0.25)	1.1568 (0.02)	1.1576 (−0.10)	1.1573 (−0.01)
Mean		1.1533 (−0.02)	1.1532 (−0.06)	1.1536 (−0.02)
St. dev.		0.0011 (0.03)	0.0011 (0.03)	0.0011 (0.02)

be discussed in the next section, confirm that these three M2 models give anomalous results in this area.

It is interesting to note that in Fig. 2, for the majority of ocean tide models, the corrected O1 has a small phase lag for most of the stations. Table 2 shows small O1 mean phase lags when GOT99.2b, NAO99b and FES99 are used for the ocean tide loading corrections. No similar phase lag for M2 is evident in Fig. 2 owing to the larger spread of results when using different ocean tide models. We will discuss the O1 phase lag further in Section 6.

6 EUROPEAN RESULTS: SUPERCONDUCTING GRAVIMETERS

Observational results are available for nine stations in Europe with superconducting gravimeters that are taking part in the Global Geo-

dynamics Project (GGP) (Crossley *et al.* 1999). These stations are listed in Table 4. The methods used for amplitude and phase calibrations of superconducting gravimeters are reviewed by Meurers (2001). Tidal analysis results have been published by the GGP databank (Ducarme & Vandercoilden 2000). In this work we have also used the results from the dual-sphere superconducting gravimeter CD029 at Wettzell (Harnisch *et al.* 2000) and the results from SG C023 at Medicina, Italy (Schwahn *et al.* 2000) and SG T018 at Potsdam (Dittfeld 2000).

The M2 and O1 observed gravimetric factors corrected for ocean tide loading and attraction using the 10 different ocean tide models are shown in Fig. 3 and the corresponding corrected phases are shown in Fig. 4. Tables 4 and 5 give the corrected gravimetric factors and phases using three of the most recent ocean tide models, GOT99.2b, NAO99b and FES99. From Fig. 3 it is immediately
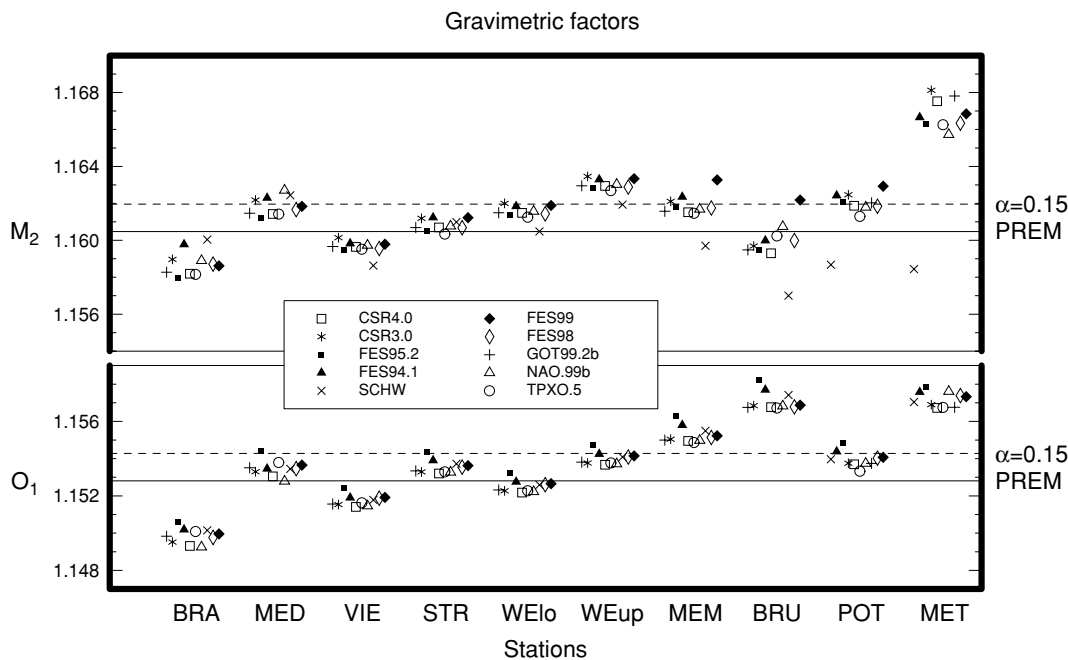

Figure 3. M2 and O1 observed gravimetric factors corrected for ocean tide loading and attraction using 10 different ocean tide models. The theoretical body tide gravimetric factors are shown for the DDW elastic PREM model and the DDW inelastic model (with $\alpha = 0.15$). The observations are from GGP superconducting gravimeters at the following sites: Brasimone (BRA) and Medicina (MED) in Italy; Vienna (VIE) in Austria; Strasbourg (STR) in France; Wettzell (WElo and WEup, where lo and up refer to the lower and upper sphere of the dual sphere SG) and Potsdam (POT) in Germany; Membach (MEM) and Brussels (BRU) in Belgium; Metsähovi (MET) in Finland.
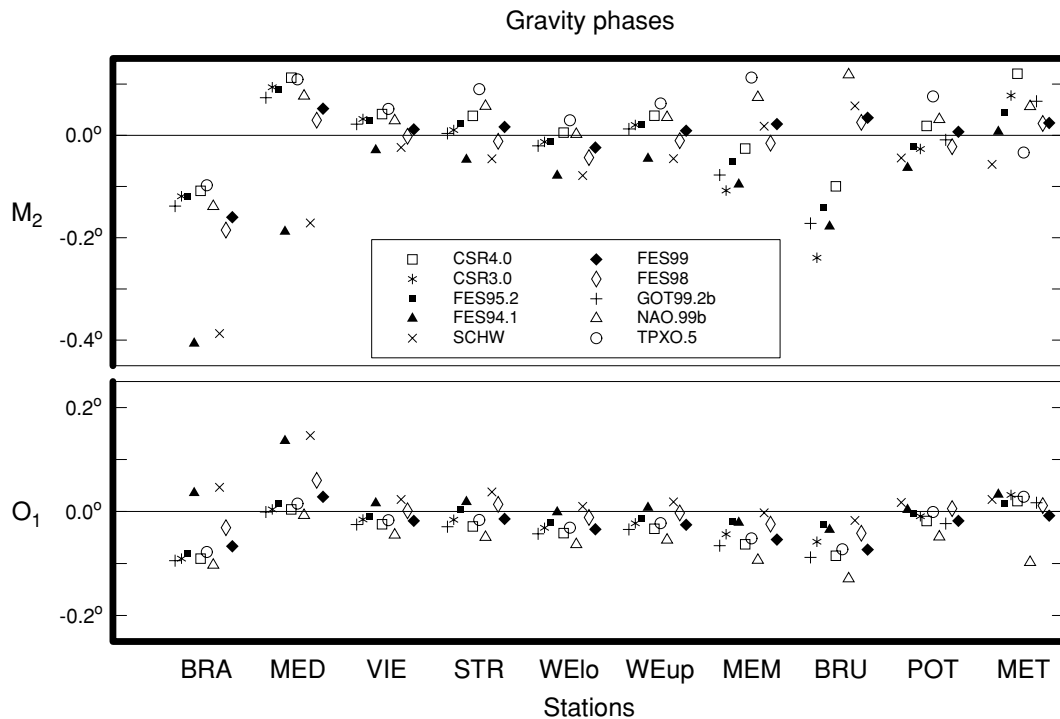
Gravity phases

Figure 4. M2 and O1 observed phases corrected for ocean tide loading and attraction using 10 different ocean tide models.

Table 5. M_2 gravimetric factors and phases: observed and observed corrected using three recent ocean tide models (local phases in degrees, lags negative).

Site	M_2 observed	Corrected using GOT 99.2b	Corrected using NAO 99b	Corrected using FES 99
Brasimone	1.1780 (1.16)	1.1583 (-0.14)	1.1589 (-0.14)	1.1586 (-0.16)
Medicina	1.1811 (1.32)	1.1615 (0.07)	1.1627 (0.08)	1.1618 (0.05)
Vienna	1.1810 (1.08)	1.1597 (0.02)	1.1597 (0.03)	1.1598 (0.01)
Strasbourg	1.1865 (2.14)	1.1607 (0.00)	1.1608 (0.06)	1.1612 (0.02)
Wettzell (lo)	1.1849 (1.38)	1.1615 (-0.02)	1.1616 (0.00)	1.1619 (-0.02)
Wettzell (up)	1.1864 (1.41)	1.1629 (0.01)	1.1630 (0.04)	1.1633 (0.01)
Membach	1.1899 (2.37)	1.1616 (-0.08)	1.1617 (0.07)	1.1633 (0.02)
Brussels	1.1839 (2.71)	1.1595 (-0.17)	1.1607 (0.12)	1.1622 (0.03)
Potsdam	1.1860 (1.36)	1.1620 (-0.01)	1.1618 (0.03)	1.1629 (0.01)
Metsähovi	1.1818 (0.73)	1.1678 (0.07)	1.1657 (0.06)	1.1668 (0.02)
	Mean	1.1614 (0.01)	1.1616 (0.05)	1.1620 (0.02)
	St. dev.	0.0010 (0.05)	0.0011 (0.03)	0.0013 (0.02)

evident that at Metsähovi both the O1 and M2 amplitudes are anomalously high by approximately 0.3 per cent. Similarly, the O1 and M2 amplitudes at Brasimone are anomalously low by approximately 0.3 per cent. This suggests calibration errors of the order of 0.3 per cent for the gravimeters at these sites. At Brussels the O1 gravimetric factor is anomalously high by approximately 0.3 per cent, which again suggests a calibration error. The anomaly is not so apparent in the M2 gravimetric factor at Brussels, but this station is only 90 km from the North Sea and the results are particularly sensitive to the loading correction (see also Fig. 4). It should be noted that for the dual-sphere superconducting gravimeter at Wettzell, the upper sphere gives gravimetric factors that are 0.13 per cent larger than the gravimetric factors for the lower sphere. These were both calibrated at the same time on the inertial sinusoidal acceleration system (Richter *et al.* 1995), which shows the technical difficulties of achieving calibration accuracies of 0.1 per cent.

In Tables 4 and 5 the mean O1- and M2-corrected gravimetric factors and standard deviations are given using the GOT99.2b, NAO99b and FES99 ocean tide models, but excluding the anomalous results at Brasimone, Brussels and Metsähovi. The mean O1-corrected gravimetric factors are in the range 1.1532–1.1536 and the mean M2-corrected gravimetric factors are in the range 1.1614–1.1620. These are between 0.06 and 0.1 per cent larger than the corrected gravimetric factors using the spring gravimeters. It should be noted that the standard deviations (after removing the above anomalous stations) are approximately 0.1 per cent.

It is clear from Fig. 4 that the superconducting gravimeter at Brasimone has an instrumental phase lag. It should also be noted that FES94.1 and Schwiderski do not include tides in the Mediterranean Sea and this causes the offsets of the results for Brasimone and Medicina using these models. Comparing Figs 4 and 2, it can be seen that several of the superconducting gravimeter stations give a

small phase lag for O1 for the majority of ocean tide models, as was the case for the spring gravimeters. Table 4 shows the small mean O1 phase lags when GOT99.2b, NAO99b and FES99 are used for the ocean tide loading corrections. A phase lag of ∼0.02° for the gravity tide is consistent with the O1 body tide model results of Mathews (2001). It is also consistent with the estimate of Ray *et al.* (2001) of 0.20° for the phase lag of the body tide Love number *k*2 using satellite laser ranging data. However, the model results of Dehant & Zschau (1989) give a phase lag of only 0.005° for tidal gravity. Melchior (1989) obtained a phase lag of 0.38° using tidal gravity measurements from 292 stations in the ICET databank. This very high phase lag reflects the significantly larger observational errors in the majority of tidal gravity measurements that were available at that time.

The residual phasor, **X**, is defined as the remaining discrepancy between an observed tidal harmonic and the total theoretical tidal gravity, which is computed by combining the theoretical body tide with the loading and attraction computed using a particular ocean tide model, i.e.

$$\mathbf{X} = \mathbf{O} - \mathbf{B} - \mathbf{L} \qquad (2)$$

where **O** is the observed tidal harmonic, **B** is the body tide computed using the DDW elastic PREM model and **L** is the ocean tide loading

and attraction computed using eq. (1). Fig. 5 shows the O1 and M2 residual phasors using the GOT99.2b and CSR4.0 ocean tide models.

It is clear that the residuals in Fig. 5 are not randomly distributed around the origin. There is a greater spread along the in-phase (real) axis, particularly for O1. For the above spring gravimeters the residuals are more randomly distributed around the origin (Baker & Bos 2001). This indicates that there are still significant calibration errors for the superconducting gravimeters in Europe. The calibration errors for the largest in-phase outliers, i.e. Brasimone, Metsähovi and Brussels have already been mentioned above. Meurers (2001) reviews the reported calibration uncertainties for superconducting gravimeters using absolute gravimeters and shows that most are in the range 0.1–0.4 per cent. In contrast, the spread of the O1 out-of-phase (imaginary) residuals in Fig. 5 is much smaller and this shows that the instrumental phase lags are now relatively well determined. The phase lags caused by the feedback, filters and data acquisition system can now be very accurately determined using the step response or injected sine waves (Van Camp *et al.* 2000). The −0.02 µGal mean bias of the O1 out-of-phase residuals in Fig. 5 is equivalent to the small phase lag discussed previously in connection with Fig. 4. It should be noted that the O1 residuals in Fig. 5 are nearly independent of the particular ocean tide model used for the
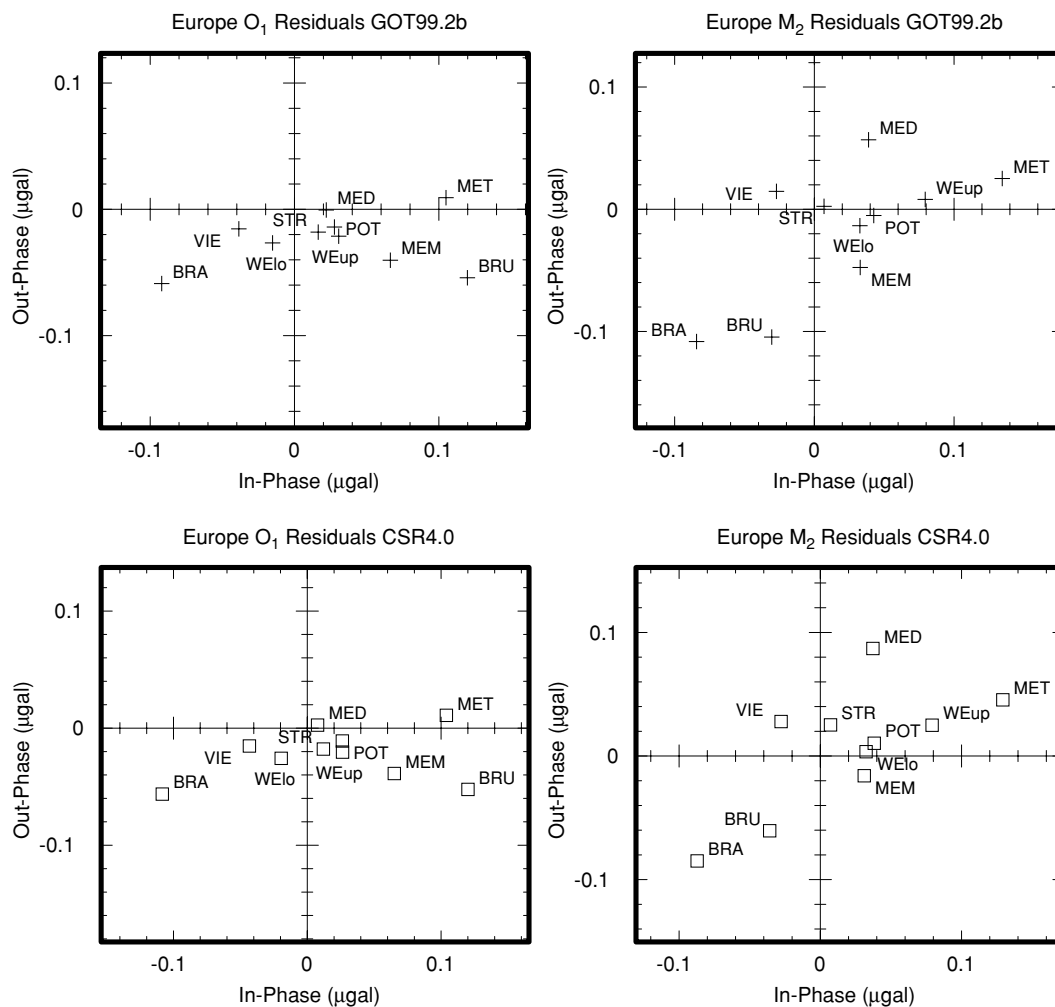

Figure 5. O1 and M2 residual phasors for European superconducting gravimeter observations using (a) the GOT99.2b ocean tide model and (b) the CSR4.0 ocean tide model. In all the phasor plots, the phase leads with respect to the tidal potential in the local meridian are plotted anticlockwise from the positive real axis.

corrections. This means that the small (0.15 μGal) O1 ocean tide loading is now very well determined in central Europe. It is very unlikely therefore that the remaining scatter in the O1 residuals can be explained by ocean tide loading. The scatter is therefore probably caused by small observational errors. Lateral heterogeneities in the Earth's body tide could also affect the residuals, but their magnitudes are generally very small. Wang (1991) shows that models of the lateral heterogeneities in the Earth's mantle from seismic tomography up to degree and order eight affect both the in-phase and out-of-phase components. He finds that the maximum effects globally are of the order of 0.03 μGal (assuming no amplification from seismic to tidal periods). However, in Europe his model gives effects that are significantly less than 0.01 μGal and are therefore too small to influence the results presented here.

The M2 residuals in Fig. 5 are more dependent than O1 upon the particular ocean tide model that is used for the corrections, as would be expected from the factor of 10 greater magnitude of the M2 loading. Since the O1 results show that the phase calibrations are relatively well determined, the out-of-phase M2 residuals can be used to discriminate between different ocean tide models. The M2 phases in Fig. 4 confirm that TPXO.5, NAO99b and FES94.1 give anomalous results at many of the European stations (see Section 5). For example, Membach is at a similar distance from the North Sea as Hannover and again gives anomalous phases using these three models. CSR3.0 also gives an anomalous phase at Membach, but this is considerably reduced with the newer version, CSR4.0.

Fig. 6 shows the O1 and M2 residuals for Wettzell (lower sphere) for all 10 ocean tide models. This is taken as being representative of a typical central European tidal gravity station and the residuals using the 10 different ocean tide models can be used to assess the magnitude of the present uncertainties in ocean tide loading in this area. For M2, Schwiderski is an obvious anomaly, as mentioned previously. The spread for O1 is approximately ±0.02 μGal for both the real and imaginary components. The M2 residuals have a similar small spread in the real component, but a higher spread in the imaginary component mainly caused by the FES94.1 and

TPXO.5 residuals. The residuals are less than 0.05 μGal in magnitude and for the majority of the European superconducting and spring tidal gravity stations discussed here the M2 and O1 residuals are less than 0.1 μGal. These are much smaller than the typical 0.3–0.6 μGal residuals found in previous work using earlier tidal gravity observations from the ICET databank (Melchior & Francis 1996; Llubes & Mazzega 1997). This illustrates the significant improvement in accuracy of the tidal gravity observations used in the present work.

7 WUHAN AND CURITIBA RESULTS: LACOSTE ET GRAVIMETERS

Wuhan is the fundamental tidal gravity station in China and similarly Curitiba in Brazil is the fundamental tidal gravity station for South America (Melchior 1994). Measurements have been made with well-calibrated LCR ET gravimeters at these fundamental stations. The ET gravimeters used at each station and the observed O1 and M2 gravimetric factors and phases are given in Table 6. The ET15 measurements in Wuhan and the ET10 measurements in Curitiba were made by the Proudman Oceanographic Laboratory. The ET16 measurements in Wuhan were made by the University of Darmstadt, FRG (Dittfeld *et al.* 1993) and the ET21 measurements were made by the Institute of Geodesy and Geophysics, Wuhan (Hsu *et al.* 1991). ET15 and ET10 have been calibrated on the Hannover vertical baseline. ET15, ET16 and ET21 have been calibrated on the Wuhan vertical baseline.

Figs 7 and 8 show the O1 and M2 gravimetric factors and phases after correcting for ocean tide loading and attraction using the 10 different ocean tide models. It is immediately evident that in comparison with Europe (Figs 1 and 2) the results are more dependent upon the choice of ocean tide model. This implies that there is a greater uncertainty in the ocean tides in these two areas. (The results for ET15 at Bad Homburg and ET16 at Potsdam are also given in Figs 7 and 8.) It can be seen that the FES series of models give the most anomalous ocean tide loading at Wuhan. Lefèvre *et al.* (2000b)
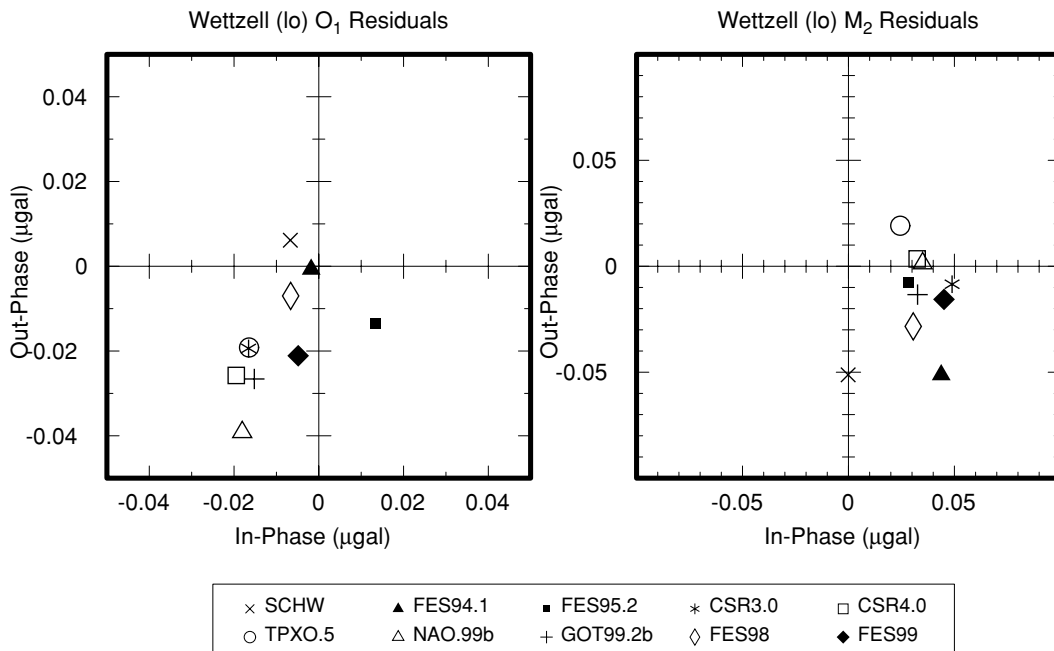

Figure 6. O1 and M2 residual phasors for Wettzell (lower sphere) using 10 different ocean tide models.

Table 6. O_1 and M_2 observed gravimetric factors and phases at Wuhan and Curitiba.

Site	Gravimeter	O_1 observed	M_2 observed
Wuhan	ET15	1.1771 (−0.41)	1.1741 (−0.41)
	ET21	1.1773 (−0.40)	1.1742 (−0.49)
	ET16	1.1752 (−0.41)	1.1720 (−0.32)
Curitiba	ET10	1.1748 (−1.12)	1.1705 (1.48)

have already discussed the difficulties of modelling the ocean tides in the relatively shallow areas of the Yellow and East China Seas and it appears that the latest versions of their model still have problems in these areas. This is particularly clear in Fig. 9, which shows the O1 and M2 residual phasors for Wuhan. For M2, the FES models give residuals between 0.2 and 0.4 μGal. For O1, FES94.1, FES98 and FES99 all give residuals greater than 0.1 μGal. The anomalous M2 Schwiderski ocean tide in the East China Sea is already well known (Hsu *et al.* 1991). It is also interesting to note that unlike CSR3.0, the CSR4.0 ocean tide model now gives results that are in very close agreement with GOT99.2b and NAO99b. For Curitiba, Figs 7 and 8 show that the M2 ocean tide models of Schwiderski, FES94.1 and FES95.2 give anomalous results. This is clearer in the Curitiba residuals in Fig. 10, where it can be seen that these three models give residuals of 0.3–0.4 μGal.

Kopaev & Kuznetsov (2000) suggest that there is strong observational evidence that the corrected gravimetric factors are approximately 0.6 per cent higher in China than Europe. However, calibration uncertainties, rather than differences in Earth structure, could explain the east–west anomaly. The LCR gravimeter ET15 has measured in both Europe (Bad Homburg) and in Wuhan and ET16 has measured in Potsdam and Wuhan. These European results are also plotted in Fig. 7 and the corrected gravimetric factors can be used to assess the possibility of any difference in the body tide gravimetric factors in the two regions. The remaining uncertainties in the ocean tide loading in Wuhan are still a problem, particularly for M2, but overall the Wuhan gravimetric factors appear to be between 0 and 0.3 per cent higher than Europe. Thus, any possible differences in gravimetric factors between Europe and China are much smaller than suggested by Kopaev & Kuznetsov (2000).

8 GLOBAL RESULTS: SUPERCONDUCTING GRAVIMETERS

In Section 6 we discussed the results from nine European stations with superconducting gravimeters that are part of the Global Geodynamics Project. In this section we will discuss the results for six GGP stations outside Europe. Tables 7 and 8 give the observed O1 and M2 gravimetric factors and phases for these GGP stations. The observational results for Cantley, Canada, are taken from Lambert *et al.* (1998) and those for Esashi, Japan, are taken from Matsumoto *et al.* (1995). The other observational results have been published by the GGP databank (Ducarme & Vandercoilden 2000).

The M2 and O1 observed gravimetric factors and phases corrected for ocean tide loading and attraction using the 10 different ocean tide models are shown in Figs 11 and 12. Tables 7 and 8 give the corrected gravimetric factors and phases using three of the most
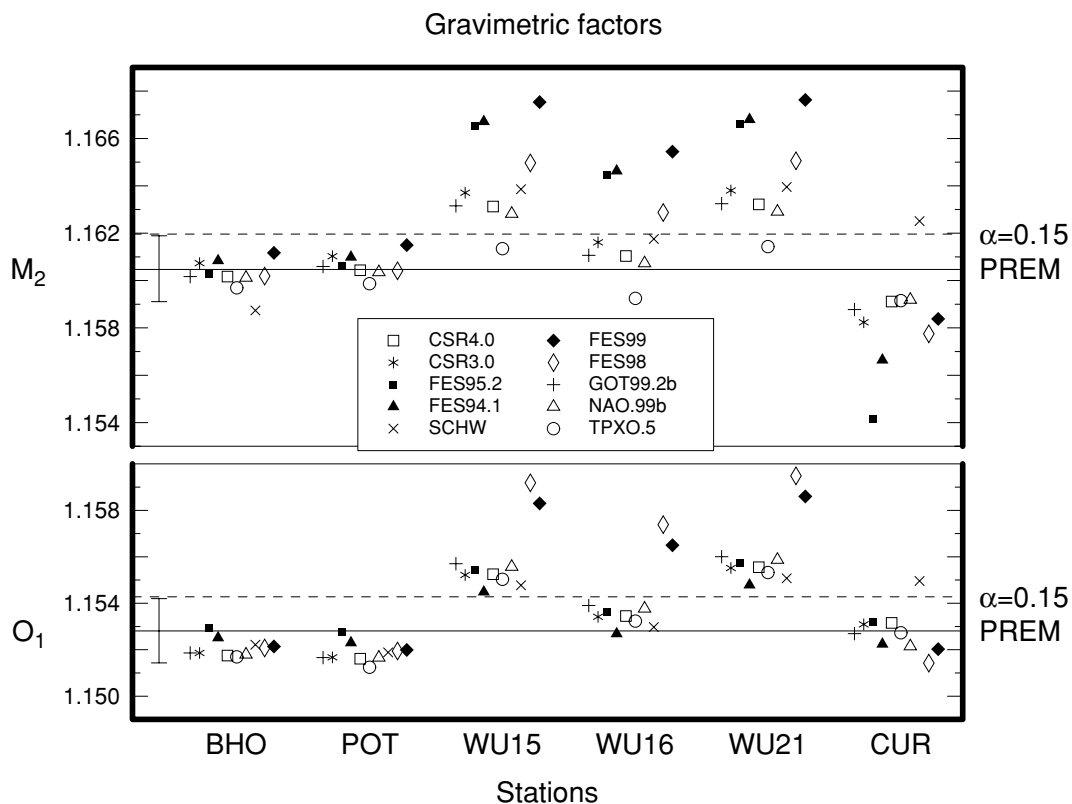

Figure 7. M2 and O1 observed gravimetric factors corrected for ocean tide loading and attraction using 10 different ocean tide models. The theoretical body tide gravimetric factors are shown for the DDW elastic PREM model and the DDW inelastic model ($\alpha = 0.15$). The observations are from the following sites and gravimeters: Wuhan, China, (WU15, WU16, WU21) with gravimeters LCR ET 15, 16 and 21, respectively; Curitiba, Brazil, (CUR) with LCR ET10. Also shown are the corresponding results from Europe with ET 15 at Bad Homburg (BHO) and ET 16 at Potsdam (POT).
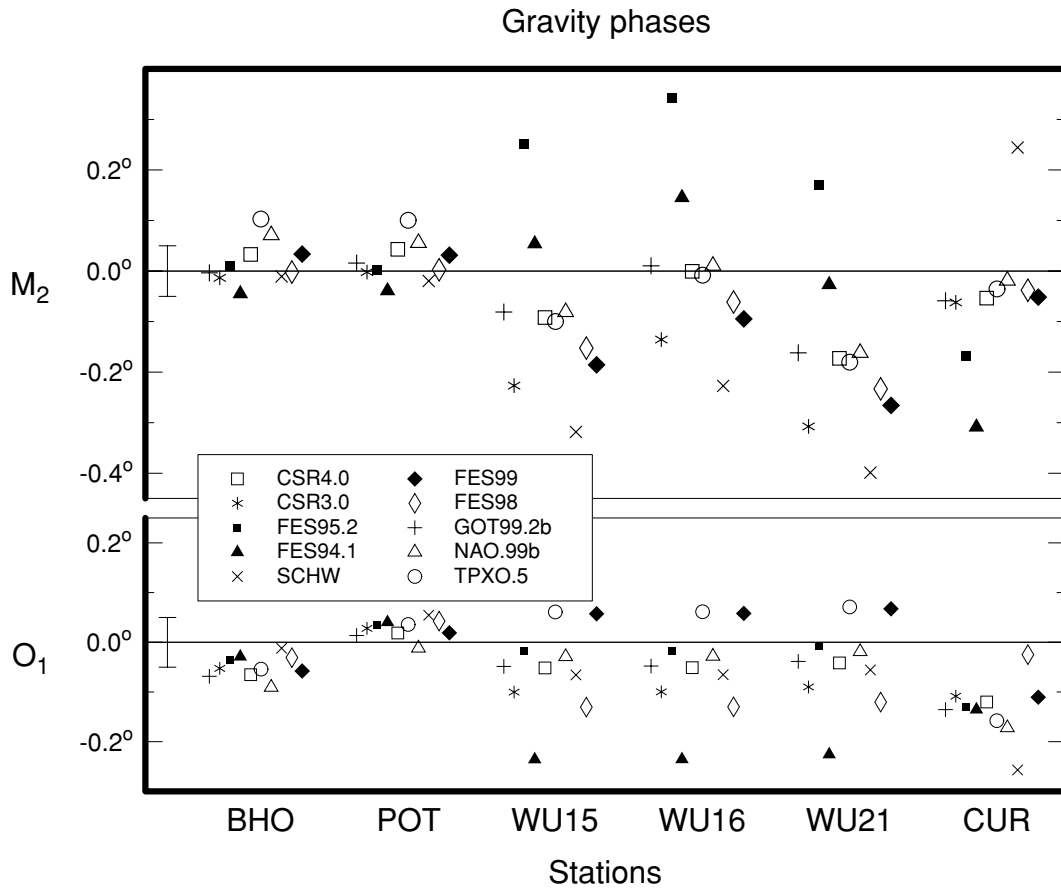
Gravity phases

Figure 8. M2 and O1 observed phases corrected for ocean tide loading and attraction using 10 different ocean tide models.
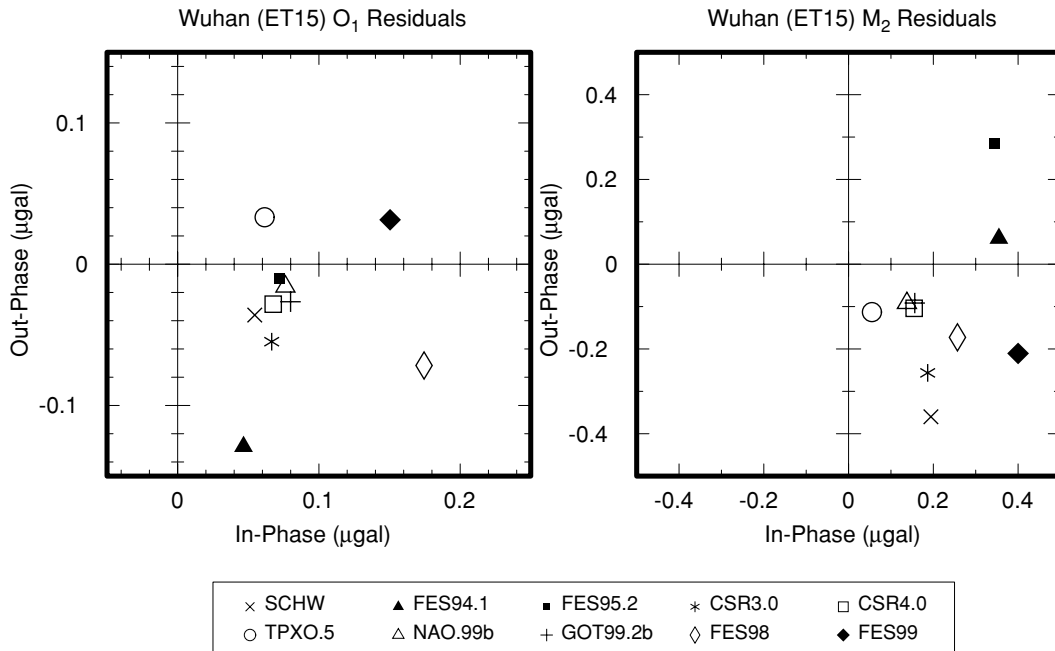

Figure 9. O1 and M2 residual phasors for Wuhan (LCR ET 15) using 10 different ocean tide models.

recent ocean tide models, GOT99.2b, NAO99b and FES99. The results for Wettzell are also plotted in Figs 11 and 12, as being representative of the results for central Europe. Again, in Figs 11 and 12 it is immediately evident that for most of the global stations the results

are more dependent upon the choice of ocean tide model than is the case for Europe. As was noted above with respect to the Wuhan LCR ET gravimeter results, the FES series of models give anomalous results for M2 with respect to other models at Wuhan, but also at Esashi
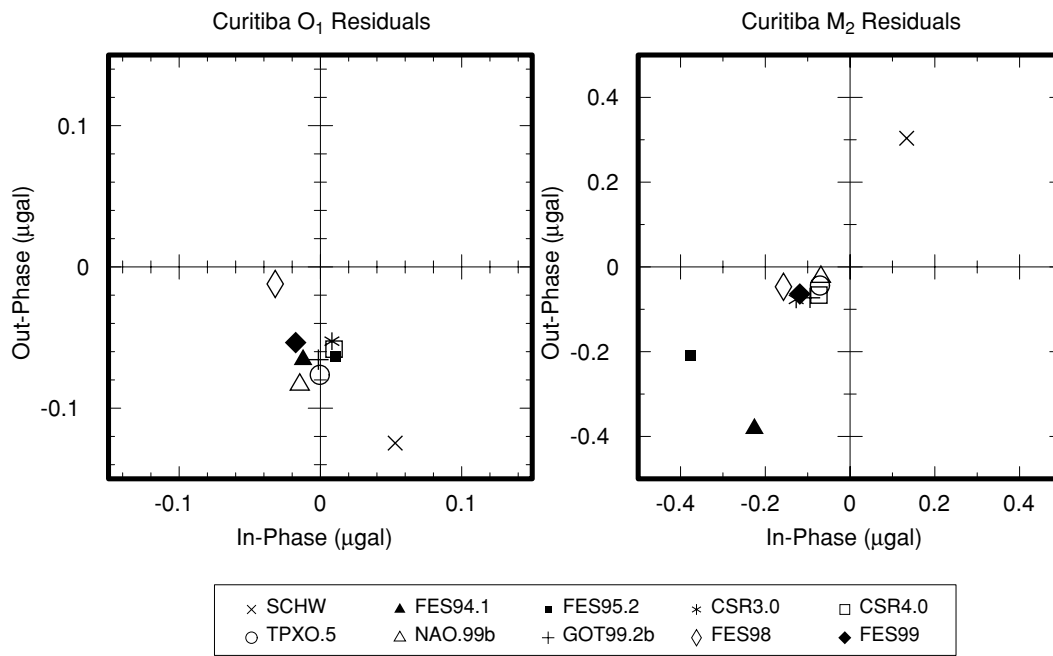
Figure 10. O1 and M2 residual phasors for Curitiba (LCR ET 10) using 10 different ocean tide models.

Table 7. O_1 gravimetric factors and phases: observed and observed corrected using three recent ocean tide models (local phases, lags negative).

Site	O_1 observed	Corrected using GOT 99.2b	Corrected using NAO 99b	Corrected using FES 99
Cantley	1.1608 (0.63)	1.1538 (0.08)	1.1537 (0.06)	1.1530 (0.06)
Boulder	1.1647 (1.32)	1.1563 (0.10)	1.1563 (0.07)	1.1562 (0.06)
Esashi	1.2201 (1.35)	1.1583 (0.08)	1.1586 (0.08)	1.1614 (0.13)
Matsushiro	1.2037 (0.69)	1.1520 (0.01)	1.1524 (0.01)	1.1556 (0.01)
Wuhan	1.1794 (−0.38)	1.1578 (−0.02)	1.1577 (0.00)	1.1605 (0.09)
Canberra	1.1742 (−0.73)	1.1551 (−0.01)	1.1551 (0.00)	1.1563 (−0.03)

Table 8. M_2 gravimetric factors and phases: observed and observed corrected using three recent ocean tide models (local phases, lags negative).

Site	M_2 observed	Corrected using GOT 99.2b	Corrected using NAO 99b	Corrected using FES 99
Cantley	1.2017 (−0.70)	1.1615 (−0.28)	1.1617 (−0.20)	1.1602 (−0.24)
Boulder	1.1594 (0.50)	1.1629 (0.00)	1.1628 (0.00)	1.1623 (−0.02)
Esashi	1.1909 (1.72)	1.1655 (0.16)	1.1655 (0.10)	1.1667 (0.08)
Matsushiro	1.1902 (0.59)	1.1598 (−0.04)	1.1599 (−0.09)	1.1610 (−0.12)
Wuhan	1.1759 (−0.26)	1.1649 (0.08)	1.1645 (0.08)	1.1693 (−0.03)
Canberra	1.1858 (−2.51)	1.1635 (0.02)	1.1639 (−0.07)	1.1610 (−0.20)

and Matsushiro. FES94.1, FES95.2 and FES99 also give anomalous M2 results at Canberra, Australia and FES94.1 gives an anomaly in the M2 phase at Boulder. For O1, again FES94.1, FES98 and FES99 give anomalous results at Wuhan, but also at Esashi and Matsushiro. FES94.1 O1 is anomalous at Canberra. The Schwiderski M2 ocean tide model gives anomalous results at Wuhan, Esashi, Matsushiro and Cantley. The Schwiderski O1 ocean tide model gives anomalous results at the two Japanese stations and also at Canberra and Boulder. Cantley, in eastern Canada has an M2 amplitude and phase that are very dependent upon the choice of ocean tide model (the O1 amplitude is also relatively dependent upon the ocean tide model). GOT99.2b, NAO99, TPXO.5, FES98 and FES99 all give reasonable corrected M2 gravimetric factors at Cantley, whereas CSR3.0, CSR4.0, FES94.1, FES95.2 and Schwiderski all give anomalously

low gravimetric factors. The M2-corrected phase at Cantley appears to be anomalous for all of the recent ocean tide models.

It is interesting to look at the O1 phases overall in Fig. 12 (ignoring the ocean tide models mentioned above, which give obvious anomalies). The corrected O1 phases at Wettzell, Matsushiro, Wuhan and Canberra are all reasonable, i.e. only a few hundredths of a degree. However, the corrected O1 phases at Cantley, Boulder and Esashi are all approximately +0.08°, which is anomalously high. There are also anomalies in some of the M2 phases, but in general the M2 results are more difficult to interpret because of the greater dependence upon the choice of ocean tide model. Similarly, looking at the gravimetric factors overall, Esashi and Wuhan show the largest departures from the PREM elastic and inelastic body tide models for both M2 and O1. If we take the DDW inelastic non-hydrostatic
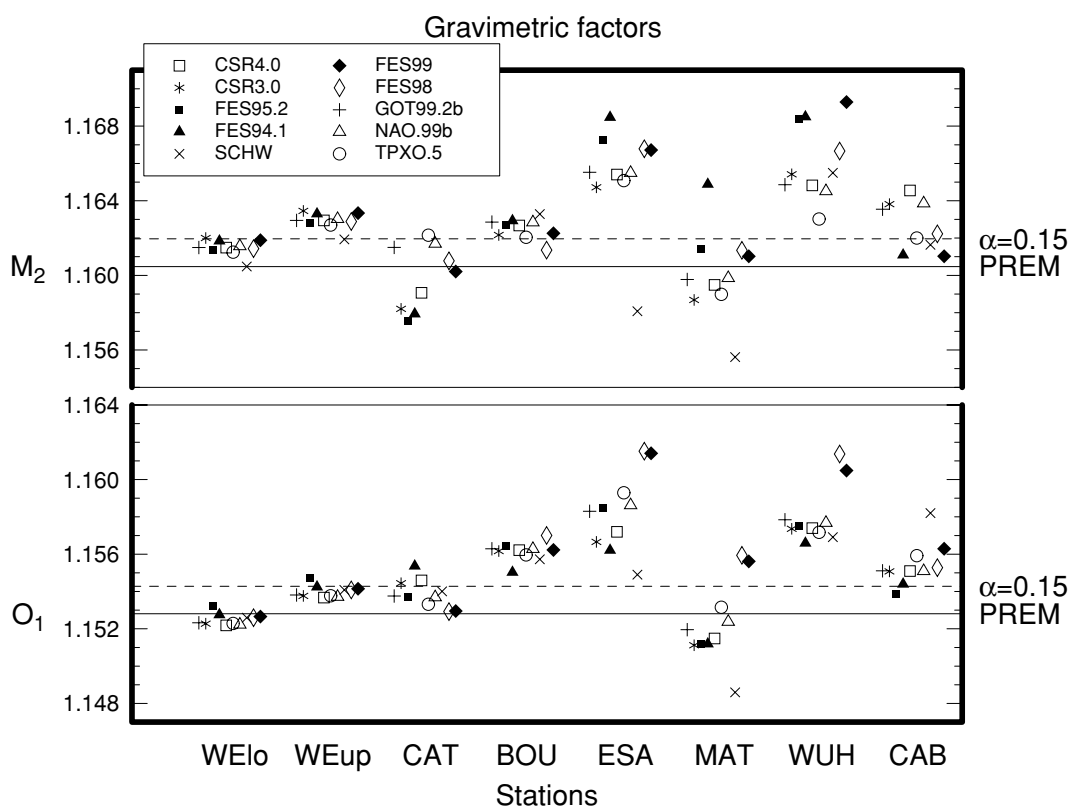
Gravimetric factors

Figure 11. M2 and O1 observed gravimetric factors corrected for ocean tide loading and attraction using 10 different ocean tide models. The theoretical body tide gravimetric factors are shown for the DDW elastic PREM model and the DDW inelastic model ($\alpha = 0.15$). The observations are from GGP superconducting gravimeters at the following sites: Wettzell (WElo and WEup) in Germany, Cantley (CAT) in Canada, Boulder (BOU) in USA, Esashi (ESA) and Matsushiro (MAT) in Japan, Wuhan (WUH) in China, and Canberra (CAB) in Australia.

body tide model as being the most realistic present-day body tide model, then the following are the typical magnitudes of the departures of the corrected O1 gravimetric factors from this model, again ignoring the ocean tide models mentioned above: Wettzell (lower) -0.15 per cent; Wettzell (upper) -0.04 per cent; Cantley -0.05 per cent; Boulder $+0.15$ per cent; Esashi $+0.3$ per cent; Matsushiro -0.2 per cent; Wuhan $+0.3$ per cent; Canberra $+0.1$ per cent. The most likely explanations for these departures from the DDW inelastic model are calibration uncertainties. This particularly applies to the larger discrepancies. Kopaev & Kuznetsov (2000) and Wang (1991) used models of lateral heterogeneities up to degree and order eight, based on seismic tomography, and found that the maximum effects on the gravimetric factors are approximately ± 0.05 per cent. It is of course possible that shorter-wavelength lateral changes in Earth structure give larger effects. Zürn *et al.* (1976) used a finite-element model to find the effects of a subducting plate on the body tide. They found that this major feature affected the vertical body tide displacement by approximately $+0.8$ per cent over the leading edge of the subducting plate and therefore, in principle, the gravimetric factor could be increased by a few tenths of a per cent (depending upon the associated change in the k Love number). Such an effect might be possible over the subducting plate under Japan. However, it should be noted that the two Japanese stations have anomalies of opposite signs. For all the tidal gravity stations, it is necessary to do further work on checking the calibrations before reaching any geophysical conclusions. For the dual-sphere superconducting gravimeter at Wettzell, despite careful calibration using inertial sinusoidal accelerations, the two spheres give gravimetric factors differing by 0.13 per cent (Harnisch *et al.* 2000). Many of the reported

calibrations using parallel recordings with an absolute gravimeter have not yet reached an accuracy level of 0.1 per cent (Meurers 2001).

Wang (1991) showed that, owing to axial asymmetry, lateral heterogeneities also cause phase shifts and that these effects are of a similar magnitude to the effects on the gravimetric factors. Fig. 13 shows the M2 and O1 residual phasors using the GOT99.2b and CSR4.0 ocean tide models. It is clear that the residuals have a greater spread along the real axis than the imaginary axis, particularly for O1. This is a further indication that amplitude calibration errors are still important. The instrumental phase lags are clearly relatively better determined than the amplitude calibrations. Since methods are now available to determine the time lag of the gravimeter system to an accuracy of 0.01 s, the imaginary component will be particularly useful for testing this component of the ocean tide models or searching for the possible effects of lateral heterogeneities.

9 CONCLUSIONS

Accurate tidal gravity measurements can be used both for testing models of the Earth's body tide and for testing the latest ocean tide models. The comparisons between observations and models presented here allow a number of conclusions to be made concerning the ocean tide models, the body tide models and the accuracy of the measurements.

Although the earlier Schwiderski (1980) ocean tide model does remarkably well in several areas, there are a number of places where it gives anomalous results. For M2, these are the gravity stations
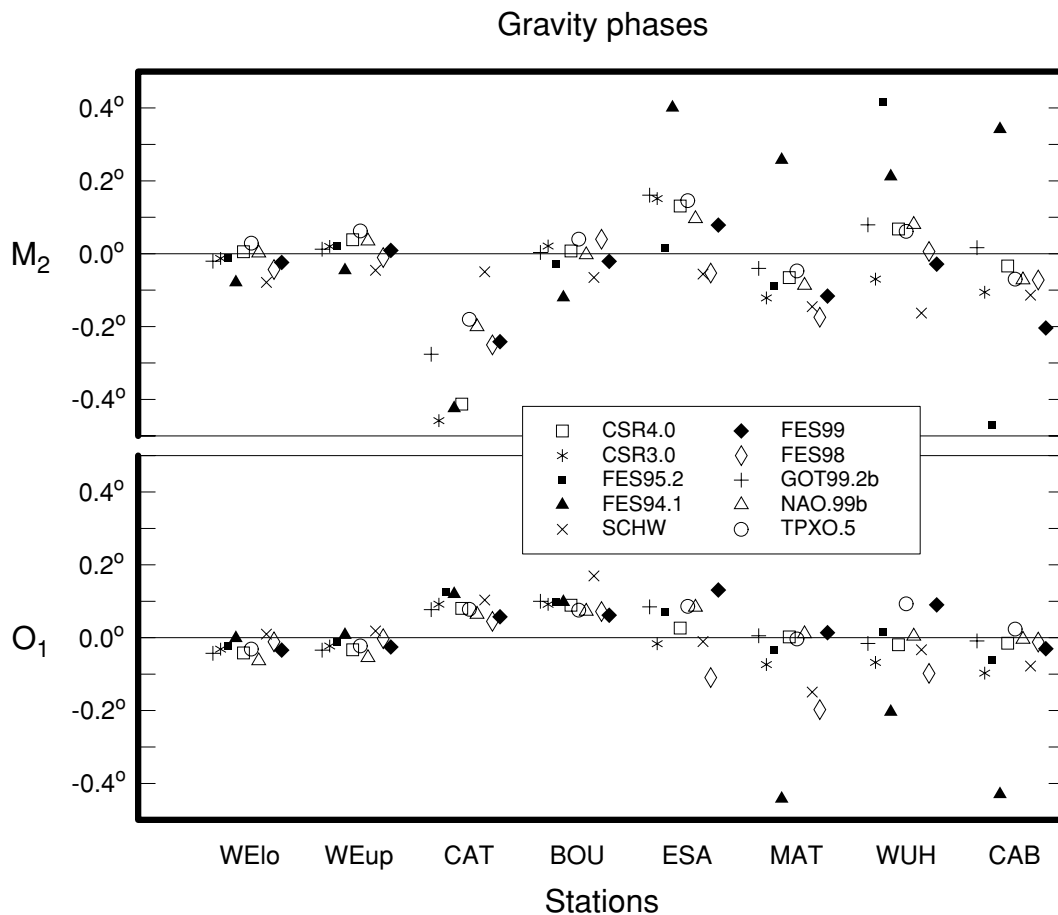
Gravity phases

Figure 12. M2 and O1 observed phases corrected for ocean tide loading and attraction using 10 different ocean tide models.

in central and northern Europe, China, Japan, Curitiba (Brazil) and Cantley (eastern Canada). For O1, Schwiderski gives anomalies in Japan, Canberra, Curitiba and Boulder. The FES94.1, 95.2, 98 and 99 M2 models give anomalous results in China and Japan and also in Canberra (with the exception of FES98). The FES94.1, FES98 and FES99 O1 models also give discrepancies in China and Japan, as does FES94.1 in Canberra. The FES94.1 and FES95.2 M2 models give anomalies in Curitiba and Cantley. In Europe, the TPXO.5, NAO99b and FES94.1 M2 ocean tide models give discrepancies, particularly for stations influenced by the North Sea. Bos *et al.* (2002) used tidal gravity measurements from Ny-Ålesund on Spitzbergen to show that FES99 is the most accurate model in the Nordic Seas. Overall, it can be concluded that the recent ocean tide models are in better agreement with tidal gravity measurements than were the earlier ocean tide models of Schwiderski and FES94.1. However, at present no single ocean tide model gives completely satisfactory results in all areas of the world.

The corrected gravimetric factors can be used for testing the body tide models, but care is needed with the interpretation of the results because of both calibration errors and the remaining uncertainties in the ocean tide loading corrections. At many stations the spread of the O1-corrected gravimetric factors and phases, using different recent ocean tide models, is smaller than the corresponding spread in M2, which makes this harmonic particularly useful for testing body tide models. In Europe, observations are available from eight stations with well-calibrated spring gravimeters and also from nine stations with superconducting gravimeters. The gravimetric factors

for the superconducting gravimeters at Brasimone, Brussels and Metsähovi are clearly anomalous, which implies calibration errors of ∼0.3 per cent at these stations. The other European stations give corrected O1 and M2 gravimetric factors that are in good agreement with the DDW elastic and inelastic body tide gravimetric factors. The estimated calibration errors at these stations are of the order of 0.1 per cent, which means that it is not yet possible to distinguish between the DDW elastic and inelastic gravimetric factors, which only differ by 0.12 per cent. However, other inelastic models with larger gravimetric factors can be rejected by these observations (see also Baker *et al.* 1996).

The majority of spring and superconducting gravimeter stations in Europe give small phase lags of a few hundredths of a degree for the corrected O1 phase, when using most of the recent ocean tide models. An O1 gravity phase lag of approximately $0.02°$ is consistent with the body tide model of Mathews (2001) and the observed $k2$ lag of Ray *et al.* (2001), but not with the model results of Dehant & Zschau (1989).

The corrected gravimetric factors for the stations outside Europe are more difficult to interpret because of the greater spread when using different ocean tide models. After discarding the obvious ocean tide model anomalies mentioned above, the corrected gravimetric factors differ from the DDW models by between -0.2 and $+0.3$ per cent. However, at this stage it would be premature to assume that these are caused by lateral heterogeneities in the Earth's structure. At many of the stations the calibration is found by parallel recording with an absolute gravimeter for a few days. Although it has been
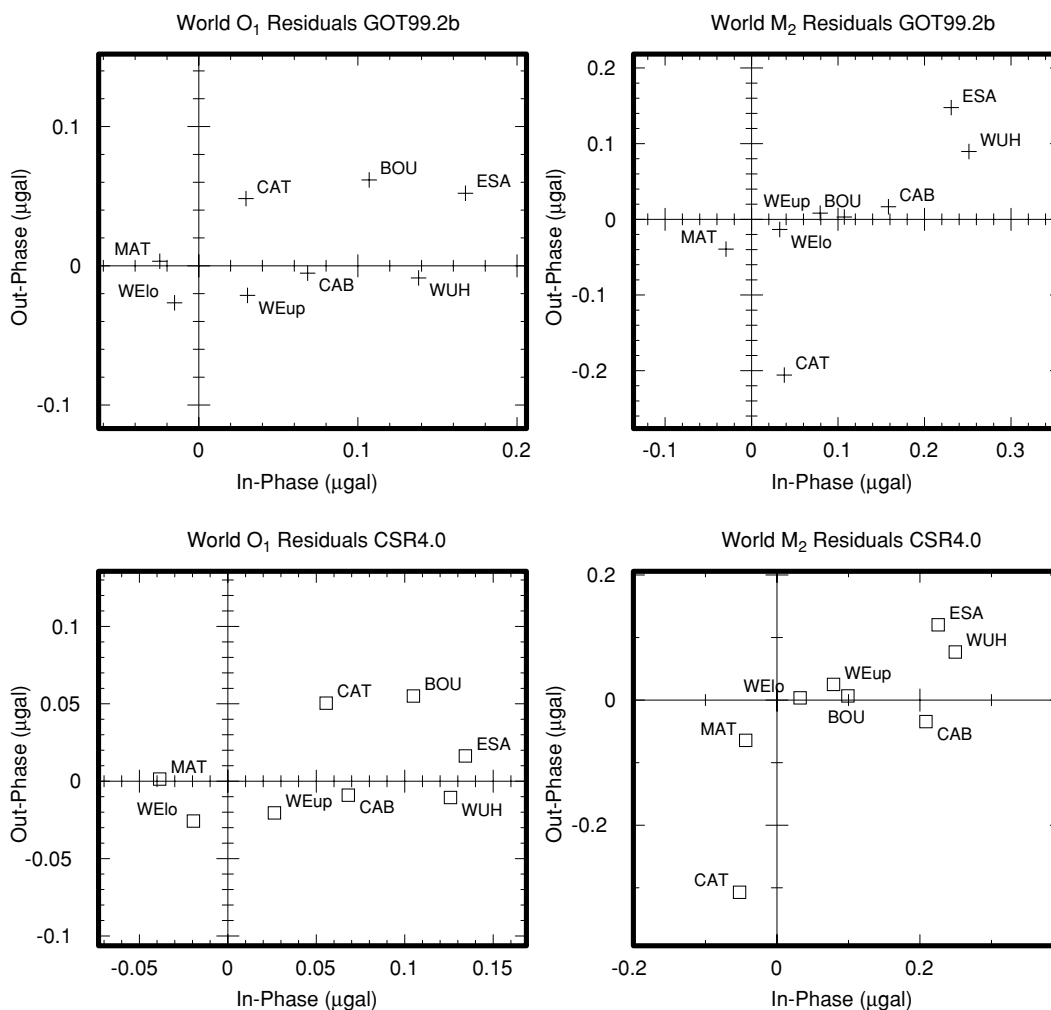
Figure 13. O1 and M2 residual phasors for GGP superconducting gravimeter observations using (a) the GOT99.2b ocean tide model and (b) the CSR4.0 ocean tide model.

clearly demonstrated that this method can achieve an accuracy of approximately 0.1 per cent, the quoted accuracy is usually between 0.1 and 0.4 per cent (Meurers 2001). It should be noted that models of lateral heterogeneities up to degree and order eight, using models from seismic tomography (and assuming no amplification from seismic to tidal periods) only predict a maximum effect of ±0.05 per cent on the gravimetric factor. Major shorter-wavelength features such as subducting plates may possibly give larger effects (Zürn *et al.* 1976), but it is clearly necessary to check and improve the calibrations before testing such models.

For the GGP superconducting gravimeter stations in Europe and the rest of the world the plots of the O1 and M2 residuals show a greater spread along the real (in-phase) axis than the imaginary axis. This shows that there are amplitude calibration problems and that the instrumental phase lags are now relatively well determined. Improved methods have been developed for accurately determining the phase lags caused by the feedback, filters and data acquisition system using the step response or injected sine waves (Van Camp *et al.* 2000). This gives the prospect of even further improvement in the imaginary component. At the same time it is proving difficult to improve the amplitude calibrations to significantly better than 0.1 per cent, despite the efforts that have been put into the use of absolute gravimeters, inertial acceleration systems and calibration masses. In the future therefore it would be an advantage to use the

significantly more accurate observations of the imaginary component. This component can be used for important tests of ocean tide models and ocean tide loading models. Also, as pointed out by Wang (1991), the axial asymmetry of lateral heterogeneities means that the effects are of a similar magnitude in the real and imaginary components and the influence on the phase of the gravity tide should be a few hundredths of a degree. The improved accuracy of the instrumental phase determinations means that it should now be possible to detect these effects in tidal gravity measurements.

ACKNOWLEDGMENTS

We would like to thank Graham Jeffries for his careful work in installing the POL LaCoste ET gravimeters in Europe, China and Brazil and the local personnel for successfully operating the instruments. In addition, we would like to thank the members of the GGP community for many stimulating discussions concerning the GGP observations at workshops over several years. Thanks are also owed to the ocean tide modellers for the early distribution of their new model solutions and to Veronique Dehant, Sonny Mathews and Rongjiang Wang for extensive discussions on the Earth's body tide models, in connection with the Working Group on theoretical tidal models.

REFERENCES

Achilli, V., Baldi, P., Casula, G., Errani, M., Focardi, S., Guerzoni, M., Palmorani, F. & Raguni, G., 1995. A calibration system for superconducting gravimeters, *Bull. Géod.,* **69,** 73–80.

Agnew, D.C., 1995. Ocean-load tides at the South Pole: a validation of recent ocean tide models, *Geophys. Res. Lett.,* **22,** 3063–3066.

Baker, T.F., 1980. Tidal gravity in Britain: tidal loading and the spatial distribution of the marine tide, *Geophys. J. R. astr. Soc.,* **62,** 249–267.

Baker, T.F. & Bos, M.S., 2001. Tidal gravity observations and ocean tide models, *J. Geodetic Soc. Japan,* **47,** 76–81.

Baker, T.F., Edge, R.J. & Jeffries, G., 1989. European tidal gravity: an improved agreement between observations and models, *Geophys. Res. Lett.,* **16,** 1109–1112.

Baker, T.F., Edge, R.J. & Jeffries, G., 1991. Tidal gravity and ocean tide loading in Europe, *Geophys. J. Int.,* **107,** 1–11.

Baker, T.F., Curtis, D.J. & Dodson, A.H., 1996. A new test of Earth tide models in central Europe, *Geophys. Res. Lett.,* **23,** 3559–3562.

Bos, M.S., Baker, T.F., Røthing, K. & Plag, H.-P., 2002. Testing ocean tide models in the Nordic Seas with tidal gravity observations, *Geophys. J. Int.,* **150,** 687–694.

Broz, J. & Simon, Z., 1997. High accurate tidal data from a Gs-15 gravimeter, *Bull. Inf. Marées Terr.,* **128,** 9893–9905.

Crossley, D. *et al.*, 1999. Network of superconducting gravimeters benefits a number of disciplines, *EOS, Trans. Am. geophys. Un.,* **80,** 121–126.

Dehant, V., 1998. Report of the Working Group on theoretical tidal models, in *Proc. 13th International Symp. on Earth Tides,* pp. 21–30, eds Ducarme, B. & Paquet, P., Observatoire Royal de Belgique, Brussels.

Dehant, V. & Zschau, J., 1989. The effect of mantle inelasticity on tidal gravity: a comparison between the spherical and the elliptical Earth model, *Geophys. J.,* **97,** 549–555.

Dehant, V., Defraigne, P. & Wahr, J.M., 1999. Tides for a convective Earth, *J. geophys. Res.,* **104,** 1035–1058.

Dittfeld, H.-J., 2000. Final results from the SG-registration in Potsdam, in *Proc. of High Precision Gravity Measurements with Application to Geodynamics and Second GGP Workshop,* Vol. 17, pp. 11–24, eds Ducarme, B. & Barthelemy, J., Cahiers du Centre Européen de Géodynamique et de Séismologie.

Dittfeld, H.-J., Becker, M. & Groten, E., 1993. Comparison of ET16 parallel recording at sites in Europe and China, *Bull. Inf. Marees Terr.,* **115,** 8484–8492.

Ducarme, B. & Vandercoilden, L., 2000. First results of the GGP databank at ICET, in *Proc. of High Precision Gravity Measurements with Application to Geodynamics and Second GGP Workshop,* Vol. 17, pp. 117–124, eds Ducarme, B. & Barthelemy, J., Cahiers du Centre Européen de Géodynamique et de Séismologie.

Dziewonski, A.D. & Anderson, D.L., 1981. Preliminary Reference Earth Model, *Phys. Earth planet. Inter.,* **25,** 297–356.

Eanes, R.J. & Bettadpur, S., 1996. *The CSR3.0 Global Ocean Tide Model: Diurnal and Semi-Diurnal Ocean Tides from TOPEX/POSEIDON Altimetry. CSR-TM-96–05,* The University of Texas Center for Space Research.

Egbert, G.D., Bennett, A.F. & Foreman, M.G., 1994. TOPEX/POSEIDON tides estimated using a global inverse model, *J. geophys. Res.,* **99,** 24 821–24 852.

Farrell, W.E., 1972a. Deformation of the Earth by surface loads, *Rev. Geophys. Space Phys.,* **10,** 761–797.

Farrell, W.E., 1972b. Global calculations of tidal loading, *Nature,* **238,** 43–44.

Francis, O., Niebauer, T.M., Sasagawa, G., Klopping, F. & Gschwind, J., 1998. Calibration of a superconducting gravimeter by comparison with an absolute gravimeter FG5 in Boulder, *Geophys. Res. Lett.,* **25,** 1075–1078.

Harnisch, M., Harnisch, G., Nowak, I., Richter, B. & Wolf, P., 2000. The dual sphere superconducting gravimeter CD029 at Frankfurt am Main and Wettzell: first results and calibration, in *Proc. of High Precision Gravity Measurements with Application to Geodynamics and Second GGP Workshop,* Vol. 17, pp. 39–56, eds Ducarme, B. & Barthelemy, J., Cahiers du Centre Européen de Géodynamique et de Séismologie.

Hinderer, J. & Crossley, D., 2000. Time variations in gravity and inferences on the Earth's structure and dynamics, *Surv. Geophys.,* **21,** 1–45.

Hsu, H.-T., Tao, G.O., Song, X.L., Baker, T.F., Edge, R.J. & Jeffries, G., 1991. Gravity tidal datum in Wuchang, China, in *Proc. 11th Int. Symp. on Earth Tides,* pp. 187–195, ed. Kakkuri, J., Schweizerbart Verlag, Stuttgart.

Kanngiesser, E. & Torge, W., 1981. Calibration of LaCoste–Romberg gravity meters, Model G and D, *Bull. Inf. Bur. Grav. Int.,* **49,** 50–63.

Kopaev, A. & Kuznetsov, F., 2000. Modelled and observed anomalies of tidal gravity factors, *Phys. and Chem. of the Earth,* **25,** 395–399.

Lambert, A., Pagiatakis, S.D., Billyard, A.P. & Dragert, H., 1998. Improved ocean tide loading corrections for gravity and displacement: Canada and northern United States, *J. geophys. Res.,* **103,** 30 231–30 244.

Lefèvre, F., Lyard, F.H. & Le Provost, C., 2000a. FES98: a new global tide finite element solution independent of altimetry, *Geophys. Res. Lett.,* **27,** 2717–2720.

Lefèvre, F., Le Provost, C. & Lyard, F., 2000b. How can we improve a global ocean tide model at a regional scale? A test on the Yellow Sea and the East China Sea, *J. geophys. Res.,* **105,** 8707–8725.

Lefèvre, F., Lyard, F.H., Le Provost, C. & Schrama, E.J.O., 2002. FES99: a global tide finite element solution assimilating tide gauge and altimetric information, *J. Atmos. Oceanic Technol.,* **19,** 1345–1356.

Le Provost, C., 2001. Ocean tides, in *Satellite Altimetry and Earth Sciences,* pp. 267–303, eds Fu, L.-L. & Cazenave, A., Academic Press, New York.

Le Provost, C., Genco, M.L., Lyard, F., Vincent, P. & Canceil, P., 1994. Tidal spectroscopy of the world ocean tides from a finite element hydrodynamic model, *J. geophys. Res.,* **99,** 24 777–24 798.

Le Provost, C., Lyard, F., Molines, J.M., Genco, M.L. & Rabilloud, F., 1998. A hydrodynamic ocean tide model improved by assimilating a satellite altimeter derived data set, *J. geophys. Res.,* **103,** 5513–5529.

Llubes, M. & Mazzega, P., 1997. Testing recent global ocean tide models with loading gravimetric data, *Prog. Oceanog.,* **40,** 369–383.

Mathews, P.M., 2001. Love numbers and gravimetric factors for diurnal tides, *J. Geodetic Soc. Japan,* **47,** 231–236.

Mathews, P.M., Dehant, V. & Gipson, J.M., 1997. Tidal station displacements, *J. geophys. Res.,* **102,** 20 469–20 477.

Matsumoto, K., Ooe, M., Sato, T. & Segawa, J., 1995. Ocean tide model obtained from TOPEX/POSEIDON altimetry data, *J. geophys. Res.,* **100,** 25 319–25 330.

Matsumoto, K., Takanezawa, T. & Ooe, M., 2000. Ocean tide models developed by assimilating TOPEX/POSEIDON altimeter data into hydrodynamical model: a global model and a regional model around Japan, *J. Oceanography,* **56,** 567–581.

Melchior, P., 1989. The phase lag of Earth tides and braking of the Earth's rotation, *Phys. Earth planet. Inter.,* **56,** 186–188.

Melchior, P., 1994. A new databank for tidal gravity measurements (DB92), *Phys. Earth planet. Inter.,* **82,** 125–155.

Melchior, P. & Francis, O., 1996. Comparison of recent ocean tide models using ground based tidal gravity measurements, *Mar. Geodesy,* **19,** 291–330.

Melchior, P. & Francis, O., 1998. Proper usage of the ICET databank: comparison with theoretical applications on Earth models, in *Proc. 13th International Symposium on Earth Tides,* pp. 377–396, eds Ducarme, B. & Paquet, P., Observatoire Royal de Belgique, Brussels.

Meurers, B., 2001. Superconducting gravimetry in geophysical research today, *J. Geodetic Soc. Japan,* **47,** 300–307.

Moore, R.D. & Farrell, W.E., 1970. Linearization and calibration of electrostatically feedback gravity meters, *J. geophys. Res.,* **75,** 928–932.

Ray, R.D., 1999. A global ocean tide model from TOPEX/POSEIDON altimetry: GOT99.2, *NASA Tech. Mem. 209478,* Goddard Space Flight Center, Greenbelt, MD. USA.

Ray, R.D., Eanes, R.J. & Lemoine, F.G., 2001. Constraints on energy dissipation in the Earth's body tide from satellite tracking and altimetry, *Geophys. J. Int.,* **144,** 471–480.

Richter, B., 1995. Cyrogenic gravimeters: status report on calibration, data acquisition and environmental effects, in *Proc. 2nd Workshop on Non Tidal Gravity Changes: Intercomparison between Absolute and Superconducting Gravimeters,* Vol. 11, pp. 125–146, ed. Poitevin, C., Cahiers du Centre Européen de Géodynamique et de Séismologie.

Richter, B., Wilmes, H. & Nowak, I., 1995. The Frankfurt calibration system for relative gravimeters, *Metrologia,* **32,** 217–223.

Schwahn, W., Baker, T.F., Falk, R., Jeffries, G., Lothhammer, A., Richter, B., Wilmes, H. & Wolf, P., 2000. Long-term increase of gravity at the Medicina station (Northern Italy) confirmed by absolute and superconducting gravimetric time series, in *Proc. of High Precision Gravity Measurements with Application to Geodynamics and Second GGP Workshop,* Vol. 17, pp. 145–168, eds Ducarme, B. & Barthelemy, J., Cahiers du Centre Européen de Géodynamique et de Séismologie.

Schwiderski, E.W., 1980. Ocean tides, Part I: global ocean tidal equations; Part II: a hydrodynamic interpolation model, *Mar. Geodesy,* **3,** 161–255.

Simon, Z. & Broz, J., 1993. Calibration of Askania gravimeter records, *Bull. Inf. Marées Terr.,* **115,** 8478–8483.

Timmen, L. & Wenzel, H.-G., 1994. Improved gravimetric Earth tide parameters for station Hannover, *Bull. Inf. Marées Terr.,* **119,** 8834–8846.

Van Camp, M., Wenzel, H.-G., Schott, P., Vauterin, P. & Francis, O., 2000. Accurate transfer function determination for superconducting gravimeters, *Geophys. Res. Lett.,* **27,** 37–40.

Wahr, J. & Bergen, Z., 1986. The effects of mantle anelasticity on nutations, Earth tides and tidal variations in rotation rate, *Geophys. J. R. astr. Soc.,* **87,** 633–668.

Wang, R., 1991. Tidal deformations on a rotating, spherically asymmetric, visco-elastic and laterally heterogeneous Earth, *PhD thesis, European University Studies, Series XVII, Earth Sciences, Vol. 5,* Peter Lang, Frankfurt am Main, p. 139.

Wenzel, H.-G., 1994. Accurate instrumental phase lag determination for feedback gravimeters, *Bull. Inf. Marées Terr.,* **118,** 8735–8752.

Wenzel, H.-G., 1996. The vertical calibration line at Karlsruhe, *Bull. Inf. Bureau Gravimetrique Int.,* **78,** 47–56.

Wenzel, H.-G., Zürn, W. & Baker, T.F., 1991. *In situ* calibration of LaCoste–Romberg Earth tide gravimeter ET19 at BFO Schiltach, *Bull. Inf. Marées Terr.,* **109,** 7849–7863.

Widmer, R., Masters, G. & Gilbert, F., 1991. Spherically symmetric attenuation within the Earth from normal mode data, *Geophys. J. Int.,* **104,** 541–553.

Zürn, W., 1997. Earth tide observations and interpretation, in *Tidal Phenomena,* Vol. 66, pp. 77–94, eds Wilhelm, H., Zürn, W. & Wenzel, H.-G., Lecture Notes in Earth Sciences, Springer, Berlin.

Zürn, W., Beaumont, C. & Slichter, L.B., 1976. Gravity tides and ocean loading in southern Alaska, *J. geophys. Res.,* **81,** 4923–4932.